encyclopedia

MDPI

Entry

Physical-Chemical Properties of Nano-Sized Phyllosilicates: Recent Environmental and Industrial Advancements

Chiara Elmi

Department of Geology and Environmental Science, James Madison University, Harrisonburg, VA 22807, USA; elmicx@jmu.edu

Definition: Phyllosilicates are common minerals that include the most widely known micas and clay minerals. These minerals are found in several natural environments and have unique physical-chemical features, such as cation exchange capacity (CEC) and surface charge properties. When phyllosilicates are nano-sized, their physical-chemical properties are enhanced from those of the micro-sized counterpart. Because of their unique crystal chemical and physical-chemical features, kinetics, and particle size, nano-sized clay minerals (i.e., kaolinite, montmorillonite/illite) and micas (i.e., muscovite) are of great interest in several fields spanning from environmental applications to engineered materials. This paper aims to overview the recent developments of environmental protection and technological applications employing nano-sized natural micas and clay minerals. Emphasis is given to the role that the unique physical-chemical properties of montmorillonite, vermiculite, kaolinite, and muscovite play in nanoparticle formulations, manufacture, and technical performance.

Keywords: phyllosilicates; nano-sized; cation exchange capacity; surface charge; applications

Citation: Elmi, C. Physical-Chemical Properties of Nano-Sized Phyllosilicates: Recent Environmental and Industrial Advancements. *Encyclopedia* **2023**, *3*, 1439–1460. https://doi.org/10.3390/encyclopedia3040103

Academic Editors: Raffaele Barretta and George Z. Kyzas

Received: 20 October 2023
Revised: 11 November 2023
Accepted: 15 November 2023
Published: 17 November 2023

1. Introduction

Phyllosilicates (from Greek *phyllon*, sheet) are the most common minerals in Earth and other planets. Phyllosilicates form a wide group that includes micas and clay minerals (Table 1). Phyllosilicates (also called layer silicates) are hydrous aluminosilicates with a structure arranged in sets of tetrahedral and octahedral sheets which are sandwiched to form a layered structure. The layered structural features provide micas and clay minerals peculiar physical-chemical properties such as cation exchange capacity (CEC), viscous and elastic capability when in contact with water, catalytic capacities, swelling behavior, and low permeability. Because of these numerous properties, phyllosilicates are of great importance in applications and innovations in mineralogy, material science, chemistry, and biomedical engineering.

Phyllosilicates are classified based on their structural features: (i) sheet types (i.e., trioctahedral or dioctahedral) and (ii) layer stacking (1:1 or 2:1). The 1:1 (or TO) layer stacking is assembled with one tetrahedral sheet and one octahedral sheet. The 2:1 (or TOT) layer stacking is built with two tetrahedral sheets sandwiching an octahedral sheet [1–3] (Figure 1). The crystal chemical features of phyllosilicates have been extensively researched in the past decades, often applying X-ray or neutron diffraction methods [1,2,4–7].

Micas and clay minerals (also called hydrous phyllosilicates) contain two-dimensional tetrahedral polymerization T_2O_5 (T = Si, Al, Fe^{3+}, etc.). Clay minerals are isostructural with micas. As in micas, clay minerals' tetrahedral (T) sheets form a hexagonal pattern and individual octahedra are generally filled with Al^{3+}, Mg^{2+}, and Fe^{2+} cations and share edges with oxygens and hydroxyl anion groups [6,7]. As in micas, clay minerals' octahedral (O) sheet can be distinguished as dioctahedral and trioctahedral. Compared to clay minerals where the interlayer can be partially occupied or can host water molecules, micas interlayer is usually fully occupied by K^+, Na^+, or Ca^{2+} in place of alkali metals [2]. Clay minerals are grouped in non-swelling (e.g., kaolinite, illite) and swelling clays (e.g., vermiculite and

smectite). It is worth noticing that many clay minerals are of finer grain sizes and lower crystallinities than most of micas. For this reason, micas are used as an approximation for the physical-chemical properties and performance of clay minerals' surfaces [8].

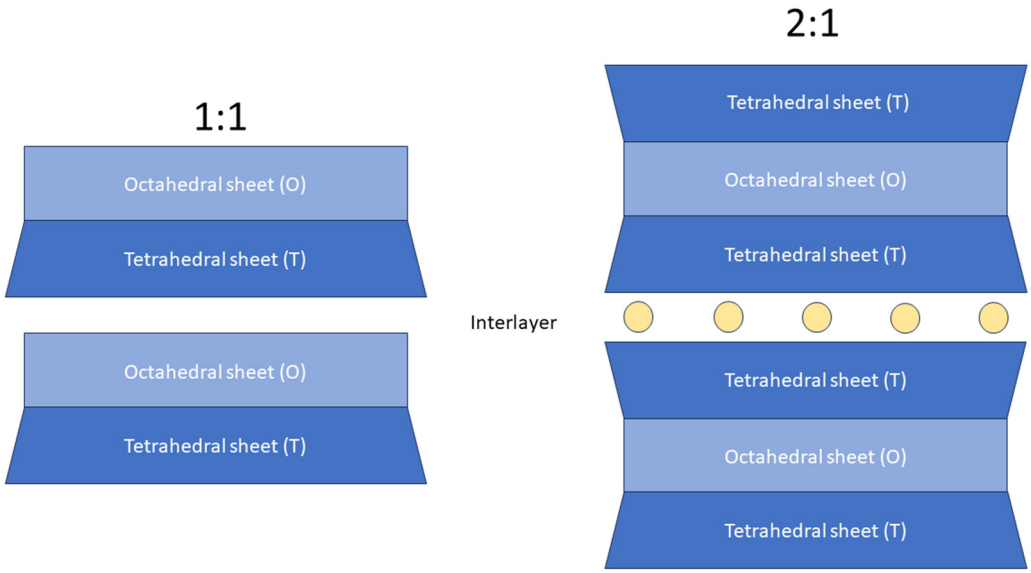

Figure 1. Schematic representation of phyllosilicate structural features. Yellow circles represent interlayer cations (commonly Na^+, K^+, Ca^{2+}).

Table 1. Endmembers of the common rock-forming mica and clay minerals groups. Data from [1,9].

Mica Group			
	Sheet Type	**Layer Stacking**	**General Formula**
Muscovite	Dioctahedral	2:1	$KAl_2(Si_3,Al)O_{10}(OH,F)_2$
Paragonite	Dioctahedral	2:1	$NaAl_2(Si_3,Al)O_{10}(OH)_2$
Margarite	Dioctahedral	2:1	$CaAl_2(Al_2Si_2)O_{10}(OH)_2$
Celadonite	Dioctahedral	2:1	$K(Mg,Fe^{3+},\square)(Si_4O_{10})(OH)_2$
Biotite	Trioctahedral	2:1	$K(Mg,Fe)_3AlSi_3O_{10}(OH,F)_2$
Phlogopite	Trioctahedral	2:1	$KMg_3(Si_3,Al)O_{10}(OH,F)_2$
Annite	Trioctahedral	2:1	$KFe_3(AlSi_3)O_{10}(OH)_2$
Lepidolite	Trioctahedral	2:1	$K(Li,Al)_3(Si,Al)_4O_{10}(OH,F)_2$
Zinnwaldite	Trioctahedral	2:1	$KLiFe^{2+}Al(AlSi_3)O_{10}(OH,F)_2$
Clay group			
Kaolinite	Dioctahedral	1:1	$Al_2Si_2O_5(OH)_4$
Halloysite	Dioctahedral	1:1	$Al_2Si_2O_5(OH)_4{\cdot}2H_2O$
Illite	Dioctahedral	2:1	$K_{0.6–0.85}(Al,Mg)_2(Si,Al)_4O_{10}(OH)_2$
Talc	Dioctahedral	2:1	$Mg_3Si_4O_{10}(OH)_2$
Pyrophyllite	Dioctahedral	2:1	$Al_2Si_4O_{10}(OH)_2$
Palygorskite	Dioctahedral	2:1	$(Mg,Al)_2Si_4O_{10}(OH){\cdot}4(H_2O)$
Sepiolite	Trioctahedral	2:1	$Mg_4Si_6O_{15}(OH)_2{\cdot}6H_2O$
Nontronite	Dioctahedral	2:1	$Na_{0.3}Fe^{3+}{}_2(Si,Al)_4O_{10}(OH)_2{\cdot}n(H_2O)$
Montmorillonite	Dioctahedral	2:1	$(Na,Ca)_{0.3}(Al,Mg)_2Si_4O_{10}(OH)_2{\cdot}nH_2O$
Vermiculite	Either trioctahedral or dioctahedral	2:1	$Mg_{0.7}(Mg,Fe^{2+},Al)_6(Si,Al)_8O_{20}(OH)_4{\cdot}8H_2O$
Glauconite	Dioctahedral	2:1	$(K,Na)(Fe^{3+}Al,Mg)_2(Si,Al)_4O_{10}(OH)_2$
Chlorite	Either trioctahedral or dioctahedral	2:1:1	$(Mg,Fe)_3(Si,Al)_4O_{10}(OH)_2{\cdot}(Mg,Fe)_3(OH)_6$

Phyllosilicates are common minerals in several oxidizing environments. Micas are widespread platy minerals found in igneous, sedimentary, and metamorphic rocks. Micas

form also as hydrothermal alteration products from the hydrolysis of feldspars [10]. Clay minerals form through the alteration of minerals such as feldspars and some ferromagnesian minerals (i.e., olivine, pyroxenes, amphiboles, etc.). The original minerals can be weathered in situ through chemical leaching caused by meteoric and ground waters and drainage. Feldspars commonly alter first to montmorillonite because the alkaline alteration environment. Montmorillonite is stable in arid climates. However, in presence of moisture, chemical leaching, and good drainage, montmorillonite alters first to halloysite and then to kaolinite. Kaolinite alters in gibbsite, if further chemical weathering occurs [11]. The alteration series of ferromagnesian minerals is: olivine → pyroxene → amphibole → biotite → chlorite → muscovite → illite. Muscovite and illite (hydro-muscovite) are commonly found in soils and residual deposits indicating a long period of weathering [11].

The widespread distribution in various Earth's crust environments and their peculiar physical-chemical properties support the impact that phyllosilicates have in different technological areas, spanning from environmental applications to nanotechnology. As raw materials, micas are used as flakes and powders in the production of fillers, cosmetics, pigments, industrial coatings, and plastics. Micas have also been used as a substrate for supporting carbon films for the study of molecular and nanoscale systems. Clays as raw materials are used in numerous industrial branches, especially in paper production, polymers, chemical and agrichemical sectors, pigments, ceramic and cement industries. Clays are also applied as fillers in pharmaceuticals, cosmetics, oil industry, civil engineering, and environmental protection projects.

Nanomaterials are rising as top materials in various fields and industries owing to their nanoscale unique performances. Mineral physical-chemical properties, kinetics, and reactivity vary as a function of particle size when smaller than a few nanometers to several tens of nanometers [12]. Nanoparticles, nanostructures, and nanosystems are developed using specific crystal chemical features by modifying their size, shape, and composition [13]. Crystal chemical properties of nano-sized natural phyllosilicates lead to their different behavior in environmental and industrial applications. Therefore, a solid crystal chemical characterization is fundamental to shed light on nanoparticles' layer charge, size, and other physical-chemical properties (e.g., colloidal suspensions, growth, adsorption, and dissolution) that are targeted in nanotechnology. Nano-sized particles show remarkable mechanical, rheological, thermal, optical, electrochemical, biodegradable, biocompatible properties that differ from those of the original micro-sized counterpart. Nanomaterials are also synthesized to enhance certain properties that can be used in applications spanning from medicine to electronics as well as energy, water, and food conservation [13,14].

Nanoclays can be defined as nanoscale clay minerals sizing from about 100 nm to a few μm. Nano-sized clay minerals include smectite (vermiculite and montmorillonite), kaolinite, and illite depending on their chemical composition and applications [15]. Nanoclays consist of TOT layer stacks of about 10 nm in size. Thus, they have approximately 657 m^2/g specific surface area compared to the micro-sized clays [16]. Nanoclays are low-cost, and nontoxic to human health or the environment. Physical, thermal, and chemical processes can produce nano-sized clays with enhanced adsorption capacity and mechanical strength [17]. Clay minerals as nano-sized units to produce nanomaterials are known as 21st-century green materials [18].

Several studies focus on using nano-sized microporous phyllosilicates owing to their high surface area, adsorption and desorption capacity, and catalytic features. The nano-sized units of clay minerals are applied to prepare functional materials shaped in nanorods, nanofibers, nanotubes, and nanosheets. Nanoclays are incorporated as matrix modifying agents to fabricate several functional green materials [13,18–22]. Kaolinite can be exfoliated into few-layered nanosheets and reassembled into functional materials with macroscopic controllable size and thus unique physical and mechanical properties [23]. Mixed-layer clay minerals (e.g., montmorillonite/illite/chlorite) can be dispersed into polymer matrices forming nanocomposites used for drug delivery carrier, food packaging, advanced rubber

and polymers [24]. Nano-sized clay minerals are mixed with organic dyes for preparing Maya Blue-like pigments [25].

This article aims to summarize the state-of-the-art of recent technological and environmental applications employing nano-sized natural micas and clay minerals with an emphasis on the importance of their physical-properties in the development of these applications. The first part of the paper outlines the methods to produce nano-sized phyllosilicates and sample preparation of phyllosilicates for X-ray powder diffraction to minimize the destruction of their structure and enhance the physical and mechanical properties. The second part of the paper reports on the most recent research progresses of technological applications employing unique physical-chemical features of the most common nano-sized phyllosilicates (montmorillonite, vermiculite, kaolinite, and muscovite).

2. Methods for Preparing Nano-Sized Phyllosilicates

2.1. Physical and Chemical Modification Methods for Preparing Nano-Sized Phyllosilicates

Several modification processes are employed to produce nano-sized natural phyllosilicates, aiming to: (1) eliminate possible impurities in the sample; (2) increase or reduce the negative surface charge; (3) increase specific surface area; (4) insert functional chemical groups or molecules in the interlayer by ion exchange process; (5) modify the morphology for increasing adsorption [26].

The most common physical methods applied to produce nano-sized phyllosilicates are ball milling, melt extrusion, ultrasonication, acid activation, and pillaring [26].

Ball milling is a mechanical method that break down clay minerals and micas aggregates. This approach performed in dry or semi-dry conditions facilities clay particles dispersion, increases specific surface area, improves adsorption efficiency, and changes the surface charge owing to the break of tetrahedral and octahedral bonds by shearing forces action [26,27]. Due to the break of tetrahedral and octahedral bonds, ball milling produces severe structural damage.

Ultrasonication produces delamination of phyllosilicates in nanometric flakes with the advantage of retaining the structure of the original micro-sized counterpart [28]. Ultrasonic delamination is performed in an aqueous suspension containing limestone. This technique is applied for producing nano-mica flakes with a 100 nm diameter-to-thickness ratio [29]. Ultrasonication method is the most valued homogenization technique for reducing particle agglomeration. Delamination of nano-phyllosilicates flakes through ultrasonication does not damage the crystal structure and enhances heat transfer performance, higher stability in fluids, and lower viscosity [30,31].

Melt extrusion is used as a pre-treatment process to produce clay–polymer nanocomposites. The process is carried out in semi-dry conditions and improves the surface area and dispersion of nano-sized clays in the polymer matrix [26,32].

Acid activation is a common chemical method for preparing functional materials starting with natural clay minerals. Acid activation involves swelling clays (i.e., montmorillonite, vermiculite) modified with a solution of HCl or H_2SO_4 for about 1 h facilitating clay particles' disaggregation, eliminating impurities (e.g., heavy metal ions), increasing the specific surface area, and adsorption property [21,26,33]. The alkaline modification can improve the adsorption capacity for pigment production because the process enhances particles' surface charge [26].

In the chemical process known as pillaring, oligomeric hydroxy-metal cations are substituted for Ca^{2+} and Na^{+}, and the mixture is then heated to temperatures higher than 300 °C. Oligomeric cations are converted into the corresponding metal oxides by heating. The newly formed metal oxides act as a nano-sized pillar in the interlayer. This method is generally applied for the adsorption of organic molecules and compounds [21].

2.2. X-ray Powder Diffraction (XRPD)

X-ray powder diffraction (XRPD) remains an essential technique for characterizing phyllosilicates. X-ray diffraction enables discoveries of new phyllosilicates and their crystal

chemical features, and provides useful information about order-disorder states, cation exchange capacity, sorption selectivity, catalytic activity, and genetic conditions [34]. The first order basal reflections are the most important for clay minerals and micas identification in a diffraction pattern. If displacements occur along both the *a* and *b* axes, the only *hkl* reflections which are possible are the basal (00*l*) reflections [35]. Table 2 reports X-ray powder diffraction basal spacing $d_{(001)}$ position of common rock-forming micas and clay minerals.

Table 2. X-ray powder diffraction $d_{(001)}$ (Å) of common phyllosilicates.

Mineral Name	$d_{(001)}$ (Å) Cu-Kα	Reference
Kaolinite	7.19	Brindley and Brown [5]
Kaolinite (disordered)	7.15	Carroll [11]
Halloysite	7.2 (dehydrated) 10.1 (hydrated)	Carroll [11]
Sepiolite	4.00–9.51 12.6, 4.31, 2.61	Brindley and Brown [5] Carroll [11]
Illite	9.91	Brindley and Brown [5]
Talc	9.32	Brindley and Brown [5]
Serpentine	8.38	Brindley and Brown [5]
Vermiculite	14.51–14.82 14.2 (unheated) 9.23 (heated) 9.3 (heated at 700 °C)	Brindley and Brown [5] Grim [35] Carroll [11]
Smectite	15.00 17.00–18.00	Carroll [11] Brindley and Brown [5]
Clinochlore [1]	14.20 13.7	Brindley and Brown [5] Grim [35]
Muscovite	10.10 9.98	Brindley and Brown [5] Grim [35]
Muscovite 1M	10.077	Carroll [11]
Muscovite 2M	10.014	Carroll [11]
Biotite	10.30 10.1	Brindley and Brown [5] Grim [35]

[1] it does not expand with Ethylene-glycol solvation.

A major problem in XRPD investigations of phyllosilicates is that samples must be prepared to minimize the destruction of the crystal structure. Commonly, sample preparation for X-ray powder diffraction requires "crushing," which is defined as an up and down motion in a mortar and pestle. The "crushing" mechanical action is far less likely to destroy phyllosilicate crystal structure. Smearing or degradation of the crystal structure of phyllosilicates lead to weak diffraction patterns or patterns that may even be nearly or functionally amorphous. The lower the crystallinity of a material, the higher the detection limit is for peaks in a given diffraction pattern. Therefore, if a phyllosilicate is present in a sample and it is not crushed, the identification may be difficult or impossible [36]. For example, talc, chlorite, smectite, and illite not properly prepared for XRD analysis can be undetected or misinterpreted in a powder X-ray diffraction pattern.

Another common method of phyllosilicates sample preparation is "grinding" which is defined as a circular motion that decreases particle size and increases reactive surface area [35]. Grinding, either in the dry or wet conditions and with the addition of chemical additives, is the common procedure used for particle size reduction and delamination of phyllosilicates to increase specific surface area and thermal behavior. However, the grinding method could damage the crystal structure of phyllosilicates leading to amorphization, or agglomeration, effects that are detrimental for several applications. It has long been recognized that grinding samples can degrade or destroy the crystal structure of phyllosilicates [37–43]. The destruction of sample crystallinity by grinding prevents accurate identification of phyllosilicates within a powdered sample. Grim [35] observed

that X-ray pattern of clay minerals ground in rubber-lined ball mill using polished agate balls showed a progressing broadening and diffuseness of the diffraction peaks with their complete amorphization after 48 h grinding indicating a gradual structure degradation.

Sonication is found to be a useful grinding method for phyllosilicates delamination. Sonication produces delamination without damaging the crystal structure, unlike other procedures such as dry grinding [30,31].

A problem arising in the identification of clay minerals in XRD patterns is the presence of mixed-layer clays. When an appropriate sample preparation and treatment protocol is employed, individual clay minerals can be uniquely identified, and the proportions of interstratified clays can also be quantified. Common intermediate products involving pure end-member clays are mixed-layer clay minerals. Mixed-layer clay minerals are abundant in nature and applied as adsorbents for the removal of heavy metals in aqueous solution owing to their large surface area and exceptional ion-exchange capacity [24]. Montmorillonite/vermiculite is a common swelling component in most mixed-layer clays. Serpentine/chlorite is a non-swelling mixed-layer clay that forms in low-temperature environments, while mica/chlorite and talc/chlorite are non-swelling mixed-layer clays that form in high-temperature environments. Moore and Reynolds [44] recognized chlorite/smectite as the second most abundant mixed layer clay mineral in sedimentary rocks, soils, and in low grade metamorphic environments. Solid state transformation and dissolution/crystallization are responsible for the formation of mixed-layer clays [45].

Mixed-layering is arranged as random, regular, or a segregation of a clay mineral inside another clay mineral [35]. In a regular mixed layering arrangement, the diffraction pattern follows a steady sequence to that of the diffraction of a single clay mineral. The structural regularity is preserved on a large scale, and a complete series of basal (00*l*) reflections is attained. The peak position and intensity of (00*l*) reflections vary with the relative abundance of different clay individuals. The structure of chlorite is an example of regular mixed layering [35]. An example of regular mixed-layer clay is rectorite, an alternation of pyrophyllite-like and montmorillonite-like layers which results in a basal spacing $d_{(001)}$ of 25 Å [11]. Random interstratification of two or three different clays is common. In random mixed layering with only a few layers of a second type present, the (00*l*) reflections do not differ from those of the dominant layer. If the second type layer is present in amounts above 10%, a series of (00*l*) reflections is obtained. Therefore, the diffraction distinction between muscovite and biotite in mixed-layer structures is not observed [35]. In a diffraction pattern, mixed layering of mica is indicated by a set of reflections on the low-angle side of the 10 Å basal spacing $d_{(001)}$. Water, when present, can be removed with heat and the structure then reverts to that of a mica; if organic matter is present, it can be removed with oxygen peroxide at 3% concentration [11].

Ethylene-glycol solvation is a standard treatment for differentiating mixed-layer clays [46]. If ethylene glycol is used, vermiculite expands to about 14.8 Å and smectite expands to about 18 Å [44]. Mixed layering of montomorillonite, vermiculite, and chlorite is evidenced by broad peaks on the high-angle side of the 14 Å basal spacing $d_{(001)}$. Glycolation and heating are common treatments for recognizing the mixed layering components that form a broad peak on the high-angle side of the 14 Å basal spacing $d_{(001)}$ [11]. In presence of a smectite/chlorite intercalation, solvation with ethylene glycol does not modify the chlorite peak position at about 14.2 Å. However, smectite expands to about 18 Å.

The distinct behaviors of K-saturated high-charge smectite and Mg-saturated vermiculite are dependent to the saturation procedure (vapor or liquid ethylene glycol) with polyalcohol. According to Mosser-Ruck et al. [47], solvation with liquid ethylene glycol is preferred in presence of mixed-layer smectite/vermiculite to separate the two components. Treatment with ethylene glycol vapor leads to either a partial or a complete lack of re-expansion of potassium-saturated smectite layers.

3. Applications and Influences

3.1. Surface Charge and Its Potential in Technological Applications

Natural phyllosilicate surface crystal structure differs from the bulk because of composition (e.g., impurities) and structure (i.e., relaxation or reconstruction processes), as well as several chemical processes (i.e., oxidation, dissolution, cation substitutions, etc.) that commonly occur in nature [48]. The physical and chemical properties of mineral surfaces can affect mineral dissolution kinetics and cation exchange capacity. Phyllosilicate's surfaces influence groundwater chemistry, organic and inorganic molecules interactions, heavy metal pollutants adsorption, etc. [8]. Muscovite is found in several empirical and technological applications derived from its bulk and surface crystal chemical features. Muscovite negatively charged surface is, for example, a perfect substratum for macromolecular growth and adsorption, or ion exchange.

The micas' surface that has been cleaved in an ambient atmosphere is very far from an inert and atomically unreactive substratum. The distribution of potassium (K^+) ions on air-cleaved muscovite has implications in several processes such as crystal growth, electrical charge transfer, and self-assembly. When cleaving a muscovite, the K^+ ions along the (001) basal plane are distributed uniformly between the two cleaved flakes, forming two neutrally charged surfaces with a K^+ each [49]. Elmi et al. [49] observed that muscovite cleaved in air may show inhomogeneities in the interlayer composition. These authors observed that the eight-fold coordination of the interlayer cation K is maintained both in the bulk and at the surface. However, the potassium amount lowered at the surface. Na substitutes K in the interlayer. The Na coordination was observed to be six at the mineral surface with an increase of the Na amount at the surface. Elmi et al. [49] concluded that the Na content in muscovite could be attributed to the presence of Na-dominant clusters in selected interlayers, as well as a solid solution mechanism (Na substitutes for K). In the cleavage region of ion-bearing phlogopites, Elmi et al. [48] observed via X-ray photoelectron spectroscopy (XPS) that the interlayer cation coordination is reduced followed by a relaxation effect. Elmi et al. [50] observed via XPS an increase in Li content on or near the (001) basal plane of a polylithionite surface. These authors observed a preference for cleavage near lithium-enriched cleaved regions.

Using grand-canonical Monte Carlo simulations, Adapa et al. [51] investigated the adsorption behavior of Li^+, Na^+, K^+, Mg^{2+}, and Ca^{2+} cations, water molecules, and role on the structural features of muscovite surface. The simulations showed that water molecules form hydrogen bonds among themselves and surface ions (Li^+, Na^+, Mg^{2+}, and Ca^{2+}) are adsorbed on the distorted hexagonal cavities near by the mica surface layers forming a balanced ordered structure.

Surface X-ray diffraction (SXRD) is a common analytical technique for exploring surfaces and interfaces [52]. Using in situ surface X-ray diffraction with crystal truncation rods (CTR), Pintea et al. [52] determined that a solid−liquid interface was formed by a muscovite interacting with $SrCl_2$ and $BaCl_2$ ionic solutions. These authors observed experimentally that the ordering is limited to the first 8–10 Å crystalline surface layer. Furthermore, adsorption of divalent ions occurs in the surface ditrigonal sites with relaxations that are close to their ionic radii.

Studying the surface charge of air-cleaved phyllosilicates is fundamental for understanding the compatibility with hydrophobic organic molecules (e.g., proteins, lipids, DNA), pharmaceuticals, pigments, selective removal of metal ions from contaminated sites and therefore opens a new pathway to prepare low-cost phyllosilicates-based functional nanomaterials with great potential.

3.2. Nano-Sized Micas for Pearlescent Pigment Production

The non-swellable layered structural property of natural micas is preferred over swellable layered structures in pigment production, owing to their homogeneous widespread horizontal length and high thermal and mechanical stability due to cation substitutions occurring in the crystal structure. The synthesis of mica pigments is based on coating

a refractive metal oxide on mica substrate (generally muscovite) that improves optical interference with visible light [53]. The metal oxides often used for coating muscovite flakes are TiO_2, Fe_2O_3, Cr_2O_3, SnO_2, ZnO, ZrO_2 [54].

Mica-titania (MT) pigment is the most common synthetic metal-oxide pearlescent pigment with iridescent and pearl-like optical effects [55]. They are not flammable and safe to human health. They are applied in cosmetics as well as in several industrial and technological products such as optical filters, printed products, polymers, stoneware, and automobile paints [30]. MT pigments are also used for printing banknotes, because the peculiar pearlescence effects make it difficult to counterfeit them by using copying machines [55]. MT pearlescent pigments are generally synthesized by depositing metal oxides onto muscovite surface. MT pigments peculiar color effect derives from light transmittance from inner muscovite substrate to outer TiO_2 coating, resulting in visible light interference and iridescent reflections [56]. Aslan et al. [57] developed MT pearlescent pigments for use in composite wall paint and observed that the synthesized pigments resulted in an enhanced pearlescent effect and lower photo-catalysis when the TiO_2 ratio increases. These authors combined MT pigments with *Chlorophytum comosum* to improve the antibacterial effect against *Escherichia coli* and antifungal effect against black mold (*Aspergillus niger*). MT pigment shows a more efficient pearlescent effect as well as anti-static and non-fading properties to ultraviolet ray if the mica substrate is coated with one or more layers of SnO_2-Sb_2O_3 (ATO) [58].

Huang et al. [59] synthesized muscovite and magnetite (Fe_3O_4) pearlescent pigment via thermal decomposition of Fe_3O_4 and formic acid. These authors found that the best conditions to obtain the optimal pearly luster effect, coating performance, and magnetic properties are a 1.0 mol/L concentration, a pH range between 4.0 and 4.5, a 3:1 formic acid/Fe^{3+} molar ratio, and a 180 rpm/min stirring speed at room temperature.

Several approaches are applied for the deposition of TiO_2 onto mica flakes, such as homogeneous hydrolysis, chemical vapor deposition, sol–gel, and calcination. The amorphous TiO_2 precipitates to crystalline TiO_2 coating when calcination occurs at 800 °C to 900 °C [54,55,60]. Štengl et al. [61] synthesized MT pigments starting with Ti, Cr, Fe, Al, Co, Ni, Zn, and Cu by homogeneous precipitation of metal sulphates with urea and by thermal annealing at temperature 150–800 °C. These authors observed that mica flake size and thickness of metal oxide deposited are the main factors affecting the performance of MT pigments as well as its chemical composition, and crystallinity. Co-precipitation calcination method is used to coat ATO on the surface of MT with sodium hydrate (NaOH) as precipitant [58]. However, ATO and MT pigment modest adhesion and downgraded pearlescent effect of MT pigments can be affected by muscovite crystal structure that could be destroyed or damaged during calcination [62].

3.3. Nanoclays and Their Role as Environmental Adsorbents

Cation exchange capacity (CEC) of clay minerals is a measure of their ability to adsorb cations from a solution. CEC depends on the crystalline structure and on the chemical composition of any solution in contact with the clay mineral. Swelling and dehydration under minor changes in temperature and water vapor pressure are important properties of clay minerals. The solid–water interface collapse and expansion in the interlayer is a unique feature that affects the transfer and fate of interlayer cations, water molecules, and pollutants. Clay minerals undergo a reversible chemical reaction known as cation exchange. This reaction occurs because of unbalanced electrical charges in the mineral framework. Either ions or water molecules in a solution in contact with the mineral surface can be replaced in the interlayer. The number of exchange sites and the strength of bonding of exchangeable cations on the mineral surface limit the cation exchange reactions. In general, the excess electrical charge on the mineral surface is negative and cations in solution are attracted to neutralize the excess electrical charge in the mineral structure [63]. The layer charge magnitude (per formula unit) is shown by CEC which ranges from 90 to 103 cmol/kg for smectites [21].

Nanoclay originates from naturally occurring clay minerals. These novel materials are receiving growing attention in recent years [64,65]. Nano-sized clay minerals are highly porous with larger surface area favoring specific cation exchange reactions at the surface owing the process of adsorption. Adsorption is the process of removing soluble materials from water, and solid adsorbents are used to adsorb pollutants in this process [64]. Modified nano-sized clays are used as adsorbents of organic pollutants in soil, water, and air as well as rheological control agents. Surface modifications of nanoclays are performed to improve tensile and strength properties as well as adsorption of contaminants [66–69]. The chemical interactions (i.e., adsorption, desorption, precipitation, dissolution, etc.) are a determining factor to initiate the mineral surface interaction with its surrounding environment.

Phenomena at the interface between soils and water are fundamental in the knowledge advance on metal corrosion, plant decontamination, heterogeneous catalysis, or soil science. Adsorption, exchange of ions with both inorganic and organic ions, binding of anions of both organic and inorganic origin, acids reaction, pillaring by various types of polyhydroxy metals, calcination, delamination by lyophilization, and ultrasound and plasma reaggregation of smectites are some of the methods used to modify the surface properties of nanoclays for environmental purposes [66].

Ion exchange is the substitution of a cation for another of a similar ionic radius on the surface or in the interstices of a crystal [70]. Intercalation with electrolyte ions modifies the surface properties of clays that are hydrophilic by nature. The hydrophilicity of nanoclays can be achieved using exchangeable hydrophilic cations and inorganic and organic molecules in the interlayer. The effective negative charged surface of nano-clay develops higher adsorption capacity on the surface with inorganic and organic contaminants in water/wastewater. Electrical conductivity properties of nanoclays are attributed to the surface electrical charge. The substitution of Al^{3+} ions for Si^{4+} in the tetrahedral layer generates a negatively charged surface. Fang et al. [71] investigated methane hydrate dissociation in clay sediments via molecular dynamics (MD) simulations. The authors attributed the phenomenon to methane nanobubbles formed at liquid water/hydrate interface.

Aromatic and phenolic pollutants can be successfully removed from groundwater by modified hybrid phyllosilicates. Such pollutants are organic compounds that are positively charged and easily attracted to the negatively charged clay surface [56]. Hybrid materials such as organo-clays can be synthesized by intercalating organic molecules into the interlayer space modifying the surface properties. The organo-montmorillonite is specifically engineered to adsorb selected organic compounds [72].

Kaolinite surface can be modified through organic and inorganic cations causing severe changes in the kaolinite crystal chemistry consequently improving its adsorption properties. The adsorption rate of nano-sized kaolinite is limited for adsorbing and removing pollutants from wastewater because its layer charge is generally close to zero [23,73].

The carboxyl-exchanged kaolinite composite is an excellent adsorbent of Ce^{3+} and other heavy metal ions from wastewater [23]. Cheng et al. [23] found that using the mechanical activation method, nano-sized kaolinite modified with amino-containing functional groups exhibited high adsorption capacity (437.6 mg/g), and faster adsorption rate. Calcination treatment of kaolinite at 550–950 °C transforms kaolinite in metakaolinite after dihydroxylation. Acid activation is a commonly used technique to increase the reactivity of adsorbents by altering their surface and increasing the rate of aluminum extraction from kaolinite octahedral layer [23,74,75].

The pH affects the adsorption capacity of nanoclays. As the pH increases, the amount of adsorbed metal ions on the kaolinite surface increases. Fida et al. [76] showed that the low pH is favorable to the Cr^{6+} removal with nano-sized kaolinite and the removal rate of Cr^{6+} reached high adsorption capacity (87%) at low pH ($pH \leq 3.0$). Nano-sized mixed-layer illite/smectite clay adsorption in aqueous solution for Cu^{2+} and Cd^{2+} ions increased (adsorption Cu^{2+} = 95.15% and adsorption Cd^{2+} = 91.53%) with increasing pH values $pH \geq 4$ [24]. The adsorption properties of mixed-layered clays for Pb^{2+} and Th^{4+} were observed to be enhanced by the presence of humic and fulvic acids which increase

adsorption of Pb^{2+} and Th^{4+} at low pH but decreased adsorption of mixed-layered clays at a basic pH [24,77,78].

Organic and aromatic micropollutants can be removed with adsorbents based on natural clay minerals. Natural clays are hydrophilic and could be ineffective for selecting hydrophobic pharmaceuticals from industrial wastewater [79,80]. Pharmaceuticals or antibiotics are efficiently removed from aqueous solutions using vermiculite. Liu et al. [81] prepared a phosphatidylcholine-intercalated vermiculite (PC-VER) for removing oxytetracycline (OTC) and ciprofloxacin (CIP) from aqueous solution. Liu et al. [81] concluded that adsorption of OTC was mainly controlled by hydrophobic interaction with PC-VER, whereas CIP adsorption is controlled by electrostatic attraction.

3.4. Importance of Nano-Sized Clay Minerals in Hazardous Waste Disposal

Geological disposal is the optimal choice for nuclear waste storage in several countries. Radioactive waste is defined as: (i) residual fuel used in nuclear power plants to generate electricity, and (ii) waste produced by nuclear weapons manufacturing facilities or spent radioactive fuel reprocessing and recycling facilities. Nuclear waste could continue to emit dangerous radioactive particles for thousands of years [82].

Clay minerals are used as a buffer surrounding the radioactive waste packages and restricting possible radioactive leakages. Bentonite and bentonite/sand mixtures are chosen mainly owing to their low hydraulic permeability in saturated conditions [83]. Swelling clays, such as smectites, are applied to seal wells in nuclear and hazardous waste repositories due to their swelling properties and adsorption capacity. Adsorption of radionuclides on nanoclays could be a major advance in reducing the transfer of radionuclides as dissolved particles from nuclear waste repositories to the environment [84]. Bentonite is a natural geological material containing mainly smectites such as montmorillonite. As it is stable over timescales of millions of years, it is used as a barrier in radioactive waste repositories [85]. The reactivity of smectite as clay barriers (CB) in deep geological storage for radioactive waste disposal is closely related to physical-chemical conditions such as pH and redox potential, high retention and swelling capacity, low permeability and diffusion, aqueous species concentrations, and/or the introduction of extraneous materials (e.g., iron, steel, concrete, glass, bitumen, etc.) [85,86].

Smectite content is also the main quality control to the mild steel corrosion. Montmorillonite absorbed water more than kaolinite, thus, it is highly effective in the deterioration of steel metals used in nuclear waste cannisters. Steel components corrode to nearly insoluble corrosion products, such as magnetite, and react with the smectite matrix in underground environments [87]. The extent of the interaction of structural Fe^{2+} and Fe^{3+} with smectite in radioactive waste repository physical-chemical conditions is poorly characterized and the thermodynamic understanding of clay mineral redox properties is still limited. Under deep repository chemical conditions, the release of Fe ions from the steel vessel can affect the physicochemical properties of the bentonite barrier through ion exchange in the interlayer [88]. Goski et al. [89] highlights the complexity of Fe redox reactions involving natural Fe-bearing smectite (Fe = 12.6 wt%) using mediated electrochemical reduction (MER) and mediated electrochemical oxidation (MEO). These authors observed that 100% structural Fe in natural smectites containing up to 12.6 wt% Fe can be quantified by MER and MEO at sufficiently low and high potential (E_H) values using appropriate mediators. Goski et al. [89] observed via spectroscopic analyses that reversible and irreversible changes in structural iron in smectites lead to changes in the standard reduction potential ($E_{H\varnothing}$) of structural iron.

Analysis of the redox properties of clay minerals is complicated by the variable reduction and oxidation of structural iron. Changes in the mineral's charge balance and differences in the size of Fe^{2+} and Fe^{3+} ions cause structural changes in the mineral. These changes result in structural differences between clay minerals in the approximately 100% Fe^{3+} oxidized state and approximately 100% Fe^{2+} reduced state, which may be partially or completely irreversible [90].

Wersin et al. [91] observed that the corrosion-derived iron (Fe) occurred predominantly in the clay matrix. Hadi et al. [92] observed that steel liner corrosion induces Fe diffusion into the bentonite, resulting in the formation of large (width > 140 mm) red, orange, and blue halos. These authors found that excess Fe^{2+} ions were adsorbed into the clay, but its speciation was ambiguously clarified. Current data suggest that ion-exchange processes may produce iron-rich smectites (e.g., saponite) or non-swelling clays (e.g., bertierine and chlorite) [87,88,91,92]. However, iron-bentonite interactions under oxidizing and reducing conditions may involve various processes such as sorption, pH changes, redox, and dissolution/precipitation reactions, the details of which are not yet understood due to limited experimental tests and physical-chemical complexity of Fe-bearing smectites.

3.5. Nanoclays in Polymers

Because of their crystal chemical properties (i.e., adsorption, CEC, high specific surface, etc.), nanoclays can be used as environmentally friendly fillers in polymeric materials. Mechanical strength and biodegradability can be improved by adsorbing small amounts of nanoscale clay particles into the polymer matrix [18,93]. Polymer–nanoclay composites are successfully applied in several fields, such as aerospace, automotive, petroleum, biomedical, construction, and wastewater treatment. Polymeric clay materials are prepared by combining polymers with nano-sized synthetic or natural clays. The clay in the polymer matrix performs as filler increasing mechanical, elastic, gas barrier properties, flame retardancy, chemical and thermal stability, recyclability of the polymer [19,22,94]. The knowledge of clay mineral crystal chemistry can facilitate the selection of the polymer matrix obtaining improved mechanical and physical properties of clay-based polymer nanocomposite systems.

Thermoplastic polyolefin (TPO) polymers are commonly reinforced with inorganic fillers because of their low cost, good processability, exceptional chemical resistance, and low density. Conventional inorganic fillers in TPOs are commonly calcite, quartz, clay minerals, micas, and talc [95,96]. The incorporation of inorganic fillers into the TPOs matrix increases thermal stability, mechanical strength (flexural and Young's moduli), and ionic conductivity of the polymer, viscoelastic properties, and reduce the cost of polymer production [96–98].

Non-flammability is an important benefit of nanoclay-polymer composite. These composites substituted the traditional halogen-containing flame retardants [19]. Several authors observed that the flame retardant properties of TPO can be improved by using modified nano-kaolinite [99–103]. The addition of nano-modified kaolinite improves fire performance for 20 wt% compared to the traditional polymeric product [23]. Sepiolite-based polymer composites have promising applications as flame-retardant and thermal-insulation material. Hu et al. [104] developed a sepiolite-based aerogel with improved mechanical properties. These authors encapsulated polyvinyl alcohol (PVA) and 3-aminopropyltriethoxysilane (KH-550) into sepiolite interlayer. Authors observed that KH-550 combined with sepiolite can effectively improve the mechanical properties and flame retardancy of aerogels, and thermal conductivity is in the range 0.0340–0.0390 W/(m·K).

Montmorillonite and laponite have potential for the design of composite membranes because increase hydrophilicity, hygroscopicity, and thermal stability of composite membranes [105]. Montmorillonite (MMT) is the mostly applied for the preparation of organoclays [94]. The interest in synthesis organoclays (OC) have obtain great attention as components forming clay polymer nanocomposites [67,94,98,106–110]. OCs such as organo-MMT are hydrophobic materials synthesized by inserting organic compounds into MMT by ion exchange and grafting methods [67]. When compared to unmodified clays, organo-MMT shows enhanced interactions with organic polymer matrices. Unmodified nanoclays do not exhibit antibacterial properties. However, when organic MMT is dispersed in an aqueous solution, microbial interactions with small antimicrobial agents embedded in clay platelets or antimicrobial polymers forming clay complexes can be increased. Several methods are employed to modify montmorillonite to produce organoclays, including ion exchange with

organic ions, surface adsorption, and grafting of organic materials. Commonly used organic modifiers include cationic, anionic, zwitterionic, nonionic and polymeric species. Organo-modification is facilitated by diverse interactions such as Van der Waals forces, cation exchange, electrostatic interactions, hydrogen bonding, and ionic dipole interactions [111].

Combining clay minerals and nano-sized polymers creates clay polymer nanocomposites (CPNs) with advanced properties that aid in the decontamination of organic and inorganic pollutants from water and wastewater [112]. Clay-polymer nanocomposites (CPNs) adsorb pollutants from water and show promising results as long-term materials in wastewater treatment [113]. Surface modification of clay minerals, especially with polymers, can significantly improve their physicochemical surface properties [95].

Naturally derived, compostable, and biodegradable polymers are suitable alternatives to single-use plastics in packaging and coating applications. However, Trinh et al. [114] observed that most sustainable polymer alternatives cannot compete with traditional plastics in gas and moisture barrier properties. Recently, improved moisture barrier properties were obtained by the encapsulation of nanoclay platelets into epoxy resin [93,95,106,115–117]. Organically modified montmorillonite is a commonly used nanoclay dispersed in epoxy resins with filling amounts ranging from 1 to 10 wt% [117].

Polylactic acid (PLA) is considered one of the best biopolymers to replace existing petroleum-based polymers in the food packaging field. PLA is derived from renewable agricultural resources such as corn, potatoes, sugar cane, and sugar beet. PLA is an environmentally friendly thermoplastic material. PLA shows a high thermal stability and good mechanical stability, but limited permeability to organic molecules, low molecular weight gases, and gases. Significant improvements in the permeability properties were observed by incorporating clay nanofillers specifically montmorillonite [118–123]. Singha and Hedenqvist [123] found that clay crystal structure can play a prominent role in the improvement of O_2 barrier properties. These authors found that exfoliation and stacking orientation of the nanoclays is the most important feature affecting PLA barrier properties. The degree of dispersion of the swelling clay minerals in the polymer matrix greatly affect the air barrier properties [123]. Enhanced dispersion was obtained by organic modification of montmorillonite interlayer sites through intercalation of organic ammonium, sulfonium or phosphonium cations [118,120,123]. Common methods for dispersing organically modified layered silicates in PLA matrices are solution incorporation, melt processing, and in situ polymerization [121]. The melt processing route is the most preferred method due to its ease of industrial implementation. This method requires mixing organically modified nanoclay with PLA and heating the mixture above the melting temperature of the polymer. High temperature and mechanical force constrain the polymer chains to diffuse into the clay interlayer, forming intercalated or exfoliated nanostructures depending on the amount of polymer chains diffused into the interlayer [119].

Functional montmorillonite can be dispersed in polymer coatings. Zhou et al. [69] reported that dispersing functional montmorillonite in polymer-based coatings can dramatically improve antibacterial activity, corrosion resistance, fire resistance, super hydrophobicity, and solar radiation absorption. Zhang et al. [124] synthesized polyaniline/organophilic montmorillonite (PANI/OMMT) composite powders and dispersed to an epoxy coating as an anti-corrosive pigment. Authors observed that the hydrophobic property and anti-corrosive property of PANI/OMMT composite was improved. Zhang et al. [124] achieved the best corrosion protection performance when 3% PANI/OMMT powder was added to the epoxy resin. Majid et al. [16] observed that addition of 3 wt% montmorillonite (MMT) nanoclay filler to the epoxy matrix of Napier/epoxy composites increased the flexural strength and flexural modulus. These authors found the highest bending strength with 163% improvement compared to traditional Napier/epoxy resin composites. Moreover, up to 180% increase in flexural modulus was achieved by adding 5 wt% nanoclay filler to the epoxy resin matrix compared to conventional Napier/epoxy resin composites.

3.6. Clay Mineral Physical-Chemical Properties for Enological Applications

Cloudiness in bottled white wine occurs because proteins in the wine become insoluble during wine storage. However, some proteins produced by yeasts can stabilize the wine [125]. Most of grape-derived proteins are pathogenesis-related (PR-proteins) with high stability to anti-proteolytic digestion and low wine pH of 3–4 [126]. Polysaccharides, polyphenols, and proteins are unstable and can promote haze formation [127]. Blade and Boulton [128] calculated protein contents in several California white wines between 20 and 260 mg/L with a mean of 116 mg/L. Thaumatin-like proteins and chitinases are PR-proteins that can also cause white wine hazing [129]. Thaumatin-like protein and chitinase show different heat stability, therefore, protein composition may impact haze formation in wines. Glucanases, thaumatines, and chitinases are the most sensitive and invertases are the least sensitive to heat-induced denaturation and precipitation treatment. This different behavior is attributed to protein crystal structural defects [130]. Thaumatin-like proteins (24 kDa fraction) contribute twice as much to the turbidity as chitinases (32 kDa fraction). Chitinases are the most sensitive to precipitation and therefore play an important role in wine haze [129].

Hazy white wines are not well valued by consumers [127,131]. Therefore, the common approach applied in enology for removing proteins is to treat wines with both organic fining agents and nano-sized bentonite. Bentonite is a phyllosilicate that belongs to the montmorillonite group. In the case of bentonite, the interlayer distance can increase to 15 Å with hydration. In the wine industry, bentonite is known as healing clay and as protein-fining agent, and because of its swelling properties can adsorb specific compounds while not influencing the quality of the wine [132]. Bentonite is commonly used to speed the settling of particulate matter, in clarifying grape juice, limiting the development of copper container oxidation, and stabilizing white wines for avoiding the hazy appearance in the bottled wine [125,130,133,134]. Because the protein content of wine is between 10 to 300 mg/L, bentonite additions range from 60 to 1800 mg/L [135]. Excessive amounts of bentonite added to wine can reduce not only proteins but also desirable wine bouquet [136]. In sparkling wine production, bentonite is typically used twice in the production process: (1) added as a fining agent to achieve protein stabilization in the base wine; (2) introduced in small amounts as an additive to the tirage solution to promote yeast flocculation [127]. Lambri et al. [136] showed that the best treatment to remove proteins without depleting wine aroma is to introduce bentonite to the grape must only. Lira et al. [125] applied a dose of 250 mg/L of bentonite at different stages of wine production (grape must clarification and beginning, middle, end of fermentation) on industrial and pilot scales. Lira et al. [125] observed that the experimental treatments affected protein stability, bouquet composition, and foam quality in white sparkling wine. Several studies indicate that there is not a standard stabilizing method applied in wine industry on the bentonite maximum amount and stage of production at which bentonite is introduced for stabilizing white wines.

For enological purposes, bentonite often preferred in the United States is the Wyoming bentonite [133]. The adsorption of positively charged proteins and other soluble cationic components by bentonite in wine is mainly due to the enhanced CEC properties of bentonite. The adsorption of a standard protein by bentonite reaches its equilibrium in less than 30 s [128]. The adsorption of thaumatin-like proteins and chitinases in bentonite interlayer is affected by pH and ethanol content of solution. Sauvave et al. [130] observed also that the thermo-sensitivity of proteins affects the adsorption capacity of bentonite.

Catarino et al. [137] carried out extraction tests of bentonites in Portuguese wines with pH value 2.94, 3.32, and 3.58. Blade and Boulton [128] carried out extraction essays of three bentonites (two Ca bentonite and a Na bentonite) on California white wine with a pH = 3.20. In both studies, authors observed a strong correlation between pH and Na content in bentonite exchange complex. The sodium bentonite is capable of adsorbing almost twice the amount of proteins than the calcium bentonite [126,128,132,137]. Because the predominant interlayer cation is sodium, the bentonite swells easily in aqueous solutions adsorbing tannins and casein.

CEC and swelling property are responsible for the enological application of bentonite. Bentonite's net negative charge attracts positively charged proteins, and the interlayer can accommodate large organic molecules, resulting in flocculation and settling as a clay–protein compound [127,129,133,135,137]. Although researchers studied alternative to bentonite [131,138], to date bentonite is still the most inexpensive and effective material applied in protein removal in the wine industry.

3.7. Clay Minerals in Healthcare

Nanoclays as functional materials has been applied in biomedical areas such as fighting and preventing of diseases. Nanoclays are active ingredients in several cosmetic products such as toothpastes, sunscreens, deodorants, moisturizers, and nail polish [139]. Talc, kaolinite, mica, and smectite are the most common modified natural and synthetic clay minerals found in cosmetic and pharmaceutical products [139,140].

The main physicochemical properties used in the cosmetic and pharmaceutical industries are surface reactivity (adsorption, cation exchange, swelling, etc.), rheology, acid absorption capacity, and solubility (HCl, H_2O). Nanoclays have small particle size, high specific surface area, and negative charge, all of which make them useful in medicine and oncology [141]. Some other natural minerals used in pharmaceutical applications are calcite, halite, and gypsum. They are abundant and cheap, and their synthesis is less complex and costly than that of clay minerals. Shahbaz et al. [142] outlined the advantages and disadvantages of using nanoclays in biomedical applications. The main disadvantages are high viscosity, agglomeration, and non-uniform distribution. However, the advantages span from structural and thermal stability to corrosion resistance, and ease manufacture.

Interlayer negative charges and the cation exchange capacity of smectites in polar media are very useful in cosmetic formulations. The absence of charged particles in talc and kaolin provides improved rheological properties and smearing effects compared to smectite [139]. Sunscreen production is another use of clays in cosmetics. Perioli et al. [143] developed a new photostable sunscreen by intercalating *p*-Aminobenzoic acid (PABA), within the lamellar structures of two kinds of hydrotalcite. Intercalated products demonstrated increased sunscreen coverage and improved photostability. Montmorillonite-supported titanium dioxide (TiO_2) composites for sunscreens were prepared by Kim et al. [144]. Authors showed that absorbance of UV by montmorillonite-TiO_2 (5:1) composites was greater than that by pure TiO_2 nanoparticles, which show nanotoxicity on skin.

Natural clays have been used since ancient times to treat skin infections. The most common nanoclays used in pharmaceutical formulation and skin pharmacy are kaolinite, talc, montmorillonite, sepiolite, and paligorskite due to their chemical inertness for the patient [141,145,146]. Kaolinite has been recently used to prepare bacterial cellulose/kaolinite nanocomposites as biomedical wound-healing materials [147]. Wanna et al. [147] observed that nano-sized kaolinite particles form a reticulated structure at kaolinite–cellulose interface and this causes the rate of blood clotting to decrease. Williams and Haydel [148] performed cation exchange experiments using Fe-smectite (French green clay), revealing an antibacterial mechanism that could provide cost-effective treatment for Buruli ulcer, a necrotizing fasciitis caused by *Mycobacterium ulcerans*. Authors observed that the pH and oxidation conditions buffered by clay mineral surfaces are key to controlling the solution chemistry and redox reactions that occur in bacterial cell walls. Superior antibacterial activity of vermiculite/chlorhexidine nanocomposites was achieved by Samlíková et al. [149]. Samlíková et al. [149] observed that the antibacterial chlorhexidine/vermiculite containing chlorhexidine ranging from 209 to 231.6 mg/g was stable with a minimum inhibitory concentration (MIC) of 3.33 (%; *w*/*v*) for *Staphylococcus aureus* after 30 h of exposure.

Recently, nanoclays have been used extensively as carriers for drugs that require delayed-release dosing owing to clays' retention capacity, swelling, and rheologic properties [145,150]. The design of drug delivery systems (DDS) is fundamental for controlling drug release and in turn reducing possible side effects in a patient. The main challenges in drug delivery are cytotoxicity, poor biodistribution, poor functionality, ineffective drug

incorporation into the delivery device, and subsequent drug release. Nanoclays are used as drug carriers for the delivery of antibiotics, antihypertensives, antipsychotics and anticancer drugs due to their excellent biocompatibility, high specific surface area, chemical inertness, colloidal and thixotropic properties [151].

Drug–nanoclay interactions depend on clay crystal structure and chemical composition. Smectites have substitutions in tetrahedral and octahedral sheets that generate a negative layer charge that can be calculated from the structural formula [1,2,152] and a pH-dependent charge limit due to oxide-like functional groups on the edge surface [153]. Because of their unique crystal chemical features, swelling clays are used as carrier materials to delay and/or release a drug and improve drug dissolution. The delayed-release dosage of a drug encapsulated into a swelling clay interlayer is related to ion-exchange mechanism and the intercalated drug amount adsorbed in the intestine that matches the cation exchange capacity (CEC) of the specific clay mineral. Krychukova et al. [80] observed that natural montmorillonite CEC to pharmaceutical varies with 97% for carbamazepine, 95% of ibuprofen, and 63–67% of paracetamol. Also, a larger specific surface area of nanoclays and the pH of the solution increase the CEC and improve the drug retention and release process [154].

Recent efforts in drug delivery include oncology. The most common nanoclays applied in oncology are kaolinite, halloysite, montmorillonite, laponite, bentonite, sepiolite, palygorskite, and allophane. Nanoclays play the role of nanocarriers improving drug dispersibility, stabilization, and transport of anticancer drugs to the tumor site [155]. In oncologic application, anticancer drug (typical drug load = 1–10 wt%) targets the tumor area in the body with a specific pharmacokinetic release profile eradicating cancer cells with an improved accuracy [156]. Methoxy-intercalated kaolinite was employed as a nanocarrier for 5-fluorouracil anticancer drug for colon-specific cancer therapy. In this application, drug molecules are usually adsorbed on the surface of kaolinite nanocomposites through hydrogen bonds, and interlayer Van der Waals forces [23].

Anionic clay, hydrotalcite Mg-Al Layered Double Hydroxides (LDH) can delay or target drug release, drug dissolution, biocompatibility, and reverse drug resistance [156]. XRD diffractogram of synthetic hydrotalcite-like anionic clays reveals sharp and intense characteristic peaks as evidence of hydrotalcite Mg-Al LDH ordered crystal structure [157]. Mei et al. [158] used hydrotalcite as a nanocarrier to integrate cancer diagnostics and therapy by adsorbing gold nanoclusters (AuNCs) and Chlorin e6 (photosensitizer, Ce6) onto the Au-doped surface of nano-sized hydrotalcite. These authors demonstrated through in vitro and in vivo therapeutic evaluations an effective driven anticancer performance of hydrotalcite Mg-Al LDH.

New trends of montmorillonite in healthcare applications concerns diabetes therapy. Rebitski et al. [154] intercalated metformin (MF), an oral drug for the treatment of type II diabetes into Wyoming montmorillonite. The intercalation amount of MF is equivalent to the CEC of montmorillonite. The incorporation of MF into montmorillonite follows an ion exchange mechanism, which increases the basal distance by 0.40 nm. Rebitski et al. [154] evaluated the montmorillonite-MF composite in gastrointestinal track pH conditions. These authors observed that the larger MF release in acidic medium requires a supplemental encapsulation into a polymer matrix to increase the MF delivery to the intestine.

4. Conclusions and Prospects

Nano-sized particles are important materials in several fields and industries. This paper reports the most recent applications of nano-sized natural micas and clay minerals that are made possible by the unique physical-chemical properties of phyllosilicates (e.g., cation exchange capacity (CEC), viscous and elastic capability when in contact with water, catalytic abilities, swelling behavior, and low permeability).

The study of crystal chemical and physical-chemical features of nano-sized micas and clay minerals aids to the advancement of technological and industrial applications. Nano-sized micas are used as flakes and powders in the production of fillers, cosmetics,

pigments, industrial coatings, and plastics. Nano-sized clay minerals are used in several industrial applications, such as ceramics, paper, polymers, dyes, and cement, as well as in pharmaceuticals, cosmetics, food, enology, petroleum industries, civil engineering, and environmental protection projects.

Nano-sized mica surfaces offer an excellent substrate for the development of pearlescent properties of pigments. Mica titanium oxide (MT) pigments are widely used in the production of cosmetics, plastics, printed products, industrial paints, and automotive paints, especially since they are non-flammable, non-self-igniting, and safe for human health. Nano-sized clay minerals have high porous property with larger surface area favoring specific cation exchange reactions owing the process of adsorption. Clay polymer nanocomposites (CPNs) have been shown to be highly efficient in adsorbing pollutants from water, showing promising results as long-term candidates for wastewater treatment. For enological purposes, nano-sized bentonite is commonly used to facilitate the settling of solid particles to avoid the appearance of haze in the bottle, when clarifying grape must, limiting oxidation of the copper container. In the healthcare field, drug-nanoclay interactions greatly depend on clay crystal chemistry. The peculiar properties of clay nanoparticles, as well as their inertness and low toxicity to human health have high potential in applications such as drug delivery. Swelling clays have been shown to improve drug retention and release because the drug or gene molecules can be safely encapsulated in the interlayer via ion exchange process.

Funding: This research received no external funding.

Institutional Review Board Statement: Not applicable.

Informed Consent Statement: Not applicable.

Data Availability Statement: No new data were created.

Acknowledgments: The author wishes to thank Mark Krekeler for suggestions and encouragements that contribute to improve the early draft of the manuscript. Anonymous reviewers are kindly acknowledged for their valuable comments that greatly improved the manuscript.

Conflicts of Interest: The author declares no conflict of interest.

References

1. Brigatti, M.F.; Galán, E.; Theng, B.K.G. Chapter 2—Structure and Mineralogy of Clay Minerals. In *Developments in Clay Science*; Bergaya, F., Lagaly, G., Eds.; Elsevier: Amsterdam, The Netherlands, 2006; Volume 5, pp. 19–86, ISBN 1572-4352.
2. Brigatti, M.F.; Malferrari, D.; Laurora, A.; Elmi, C. Structure and Mineralogy of Layer Silicates: Recent Perspectives and New Trends. In *Layered Mineral Structures and Their Application in Advanced Technologies*; Brigatti, M.F., Mottana, A., Eds.; Mineralogical Society of Great Britain and Ireland: Middlesex, UK, 2011; Volume 11, pp. 1–71, ISBN 978-0-903056-29-8.
3. Brigatti, M.F.; Guggenheim, S.J. Mica Crystal Chemistry and the Influence of Pressure, Temperature, and Solid Solution on Atomistic Models. *Rev. Mineral. Geochem.* **2002**, *46*, 1–97. [CrossRef]
4. Brigatti, M.F.; Galán, E.; Theng, B.K.G. Structure and Mineralogy of Clay Minerals. In *Developments in Clay Science*; Elsevier: Amsterdam, The Netherlands, 2013; Volume 5, pp. 21–81, ISBN 978-0-08-099364-5.
5. Brindley, G.W.; Brown, G. (Eds.) *Crystal Structures of Clay Minerals and Their X-ray Identification*; Mineralogical Society of Great Britain and Ireland: Middlesex, UK, 1980; ISBN 978-0-903056-08-3.
6. Brown, G. Structure, Crystal Chemistry, and Origin of the Phyllosilicate Minerals Common in Soil Clays. In *Soil Colloids and Their Associations in Aggregates*; De Boodt, M.F., Hayes, M.H.B., Herbillon, A., De Strooper, E.B.A., Tuck, J.J., Eds.; Springer: Boston, MA, USA, 1990; pp. 7–38, ISBN 978-1-4899-2611-1.
7. Guggenheim, S.; Martin, R.T. Definition of Clay and Clay Mineral: Joint Report of the Aipea Nomenclature and CMS Nomenclature Committees. *Clays Clay Miner.* **1995**, *43*, 255–256. [CrossRef]
8. Elmi, C.; Guggenheim, S.; Gieré, R. Surface Crystal Chemistry of Phyllosilicates Using X-ray Photoelectron Spectroscopy: A Review. *Clays Clay Miner.* **2016**, *64*, 537–551. [CrossRef]
9. Sinha Ray, S. 1—An Overview of Pure and Organically Modified Clays. In *Clay-Containing Polymer Nanocomposites*; Sinha Ray, S., Ed.; Elsevier: Amsterdam, The Netherlands, 2013; pp. 1–24, ISBN 978-0-444-59437-2.
10. Alderton, D. Micas. In *Encyclopedia of Geology*, 2nd ed.; Alderton, D., Elias, S.A., Eds.; Academic Press: Oxford, UK, 2021; pp. 326–333, ISBN 978-0-08-102909-1.
11. Carroll, D. *Clay Minerals: A Guide to Their X-ray Identification*; Special Paper; Geological Society of America: Boulder, CO, USA, 1970; ISBN 978-0-8137-2126-2.

12. Hochella, M.F.; Lower, S.K.; Maurice, P.A.; Penn, R.L.; Sahai, N.; Sparks, D.L.; Twining, B.S. Nominerals, Mineral Nanoparticles, and Earth Systems. *Science* **2008**, *319*, 1631–1635. [CrossRef]
13. Barhoum, A.; García-Betancourt, M.L.; Jeevanandam, J.; Hussien, E.A.; Mekkawy, S.A.; Mostafa, M.; Omran, M.M.; Abdalla, M.S.; Bechelany, M. Review on Natural, Incidental, Bioinspired, and Engineered Nanomaterials: History, Definitions, Classifications, Synthesis, Properties, Market, Toxicities, Risks, and Regulations. *Nanomaterials* **2022**, *12*, 177. [CrossRef]
14. Hochella, M.F.; Mogk, D.W.; Ranville, J.; Allen, I.C.; Luther, G.W.; Marr, L.C.; McGrail, B.P.; Murayama, M.; Qafoku, N.P.; Rosso, K.M.; et al. Natural, Incidental, and Engineered Nanomaterials and Their Impacts on the Earth System. *Science* **2019**, *363*, eaau8299. [CrossRef]
15. Kirbiyik Kurukavak, Ç. Thermal and Morphological Characterization of Bionanocomposites. In *Reference Module in Materials Science and Materials Engineering*; Elsevier: Amsterdam, The Netherlands, 2022; ISBN 978-0-12-803581-8.
16. Majid, M.S.A.; Ridzuan, M.J.M.; Lim, K.H. 6—Effect of Nanoclay Filler on Mechanical and Morphological Properties of Napier/Epoxy Composites. In *Interfaces in Particle and Fibre Reinforced Composites*; Goh, K.L., Aswathi, M.k., De Silva, R.T., Thomas, S., Eds.; Woodhead Publishing Series in Composites Science and Engineering; Woodhead Publishing: Sawston, UK, 2020; pp. 137–162, ISBN 978-0-08-102665-6.
17. Guan, H.; Zhao, Y. 9—Decontamination Application of Nanoclays. In *Clay Nanoparticles*; Cavallaro, G., Fakhrullin, R., Pasbakhsh, P., Eds.; Micro and Nano Technologies; Elsevier: Amsterdam, The Netherlands, 2020; pp. 203–224, ISBN 978-0-12-816783-0.
18. Wang, W.; Wang, A. Nanoscale Clay Minerals for Functional Ecomaterials: Fabrication, Applications, and Future Trends. In *Handbook of Ecomaterials*; Martínez, L.M.T., Kharissova, O.V., Kharisov, B.I., Eds.; Springer International Publishing: Cham, Switzerland, 2019; pp. 2409–2490, ISBN 978-3-319-68255-6.
19. Kausar, A. 7—Flame Retardant Potential of Clay Nanoparticles. In *Clay Nanoparticles*; Cavallaro, G., Fakhrullin, R., Pasbakhsh, P., Eds.; Elsevier: Amsterdam, The Netherlands, 2020; pp. 169–184, ISBN 978-0-12-816783-0.
20. Sinha Ray, S.; Bousmina, M. Biodegradable Polymers and Their Layered Silicate Nanocomposites: In Greening the 21st Century Materials World. *Prog. Mater. Sci.* **2005**, *50*, 962–1079. [CrossRef]
21. Theng, B.K.G.; Churchman, G.J.; Gates, W.P.; Yuan, G. Organically Modified Clays for Pollutant Uptake and Environmental Protection. In *Soil Mineral Microbe-Organic Interactions: Theories and Applications*; Huang, Q., Huang, P.M., Violante, A., Eds.; Springer: Berlin/Heidelberg, Germany, 2008; pp. 145–174, ISBN 978-3-540-77686-4.
22. Xu, P.; Qi, G.; Lv, D.; Niu, D.; Yang, W.; Bai, H.; Yan, X.; Zhao, X.; Ma, P. Enhanced Flame Retardancy and Toughness of Eco-Friendly Polyhydroxyalkanoate/Bentonite Composites Based on in Situ Intercalation of P-N-Containing Hyperbranched Macromolecules. *Int. J. Biol. Macromol.* **2023**, *232*, 123345. [CrossRef]
23. Cheng, H.; Zhou, Y.; Liu, Q. 6—Kaolinite Nanomaterials: Preparation, Properties and Functional Applications. In *Nanomaterials from Clay Minerals*; Wang, A., Wang, W., Eds.; Micro and Nano Technologies; Elsevier: Amsterdam, The Netherlands, 2019; pp. 285–334, ISBN 978-0-12-814533-3.
24. Deng, H.; Wu, Y.; Shahzadi, I.; Liu, R.; Yi, Y.; Li, D.; Cao, S.; Wang, C.; Huang, J.; Su, H. 8—Nanomaterials From Mixed-Layer Clay Minerals: Structure, Properties, and Functional Applications. In *Nanomaterials from Clay Minerals*; Wang, A., Wang, W., Eds.; Micro and Nano Technologies; Elsevier: Amsterdam, The Netherlands, 2019; pp. 365–413, ISBN 978-0-12-814533-3.
25. Dong, J.; Zhang, J. 13—Maya Blue Pigments Derived From Clay Minerals. In *Nanomaterials from Clay Minerals*; Wang, A., Wang, W., Eds.; Micro and Nano Technologies; Elsevier: Amsterdam, The Netherlands, 2019; pp. 627–661, ISBN 978-0-12-814533-3.
26. Wang, A.; Wang, W. 1—Introduction. In *Nanomaterials from Clay Minerals*; Wang, A., Wang, W., Eds.; Micro and Nano Technologies; Elsevier: Amsterdam, The Netherlands, 2019; pp. 1–20, ISBN 978-0-12-814533-3.
27. Liu, Y.; Wang, W.; Wang, A. Effect of Dry Grinding on the Microstructure of Palygorskite and Adsorption Efficiency for Methylene Blue. *Powder Technol.* **2012**, *225*, 124–129. [CrossRef]
28. Pérez-Rodríguez, J.L.; Madrid Sánchez del Villar, L.; Sánchez-Soto, P.J. Effects of Dry Grinding on Pyrophyllite. *Clay Miner.* **1988**, *23*, 399–410. [CrossRef]
29. Kauffman, S.H.; Leidner, J.; Woodhams, R.T.; Xanthos, M. The Preparation and Classification of High Aspect Ratio Mica Flakes for Use in Polymer Reinforcement. *Powder Technol.* **1974**, *9*, 125–133. [CrossRef]
30. Malayoglu, U.; Besun, N. Development of Nanosized Mica Particles from Natural Mica by Sonication/Organic Intercalation Method for Pearlescent Pigment. *Minerals* **2020**, *10*, 572. [CrossRef]
31. Pérez-Rodríguez, J.L.; Wiewióra, A.; Drapaa, J.; Pérez-Maqueda, L.A. The Effect of Sonication on Dioctahedral and Trioctahedral Micas. *Ultrason. Sonochemistry* **2006**, *13*, 61–67. [CrossRef] [PubMed]
32. Chen, J.; Jin, Y.; Qian, Y.; Hu, T. A New Approach to Efficiently Disperse Aggregated Palygorskite Into Single Crystals via Adding Freeze Process Into Traditional Extrusion Treatment. *IEEE Trans. Nanotechnol.* **2010**, *9*, 6–10. [CrossRef]
33. Barrios, M.S.; González, L.V.F.; Rodríguez, M.A.V.; Pozas, J.M.M. Acid Activation of a Palygorskite with HCl: Development of Physico-Chemical, Textural and Surface Properties. *Appl. Clay Sci.* **1995**, *10*, 247–258. [CrossRef]
34. Konta, J. Clay Minerals Including Related Phyllosilicates: Interdisciplinary Research and Inward Integration. *Acta Geodyn. Geomater.* **2005**, *2*, 53–68.
35. Grim, R.E. *Clay Mineralogy*; McGraw-Hill: New York, NY, USA, 1968; ISBN 978-0-07-024836-6.
36. Bish, D.L.; Post, J.E. (Eds.) *Modern Powder Diffraction*; Mineralogical Society of America; De Gruyter: Chantilly, VA, USA, 1989; Volume 20. ISBN 978-1-5015-0901-8.
37. Gregg, S.J.; Parker, T.W.; Stephens, M.J. The Effect of Grinding on Kaolinite. *Clay Miner. Bull.* **1953**, *2*, 34–44. [CrossRef]

38. Mackenzie, R.C.; Milne, A.A. The Effect of Grinding on Micas. I. Muscovite. *Mineral. Mag. J. Mineral. Soc.* **1953**, *30*, 178–185. [CrossRef]
39. Takahashi, H. Effect of Dry Grinding on Kaolin Minerals. *Clays Clay Miner.* **1957**, *6*, 279–291. [CrossRef]
40. Miller, J.G.; Oulton, T.D. Prototropy in Kaolinite during Percussive Grinding. *Clays Clay Miner.* **1970**, *18*, 313–323. [CrossRef]
41. Čičel, B.; Kranz, G. Mechanism of Montmorillonite Structure Degradation by Percussive Grinding. *Clay Miner.* **1981**, *16*, 151–162. [CrossRef]
42. Cornejo, J.; Hermosin, M.C. Structural Alteration of Sepiolite by Dry Grinding. *Clay Miner.* **1988**, *23*, 391–398. [CrossRef]
43. Reynolds, R.C., Jr.; Bish, D.L. The Effects of Grinding on the Structure of a Low-Defect Kaolinite. *Am. Mineral.* **2002**, *87*, 1626–1630. [CrossRef]
44. Moore, D.M.; Reynolds, R.C., Jr. *X-ray Diffraction and Identification and Analysis of Clay Minerals*, 2nd ed.; Oxford University Press: New York, NY, USA, 1997; ISBN 978-0-19-508713-0.
45. Środoń, J. Nature of Mixed-Layer Clays and Mechanisms of Their Formation and Alteration. *Annu. Rev. Earth Planet. Sci.* **1999**, *27*, 19–53. [CrossRef]
46. Brindley, G.W. Ethylene Glycol and Glycerol Complexes of Smectites and Vermiculites. *Clay Miner.* **1966**, *6*, 237–259. [CrossRef]
47. Mosser-Ruck, R.; Devineau, K.; Charpentier, D.; Cathelineau, M. Effects of Ethylene Glycol Saturation Protocols on XRD Patterns: A Critical Review and Discussion. *Clays Clay Miner.* **2005**, *53*, 631–638. [CrossRef]
48. Elmi, C.; Brigatti, M.F.; Guggenheim, S.; Pasquali, L.; Montecchi, M.; Nannarone, S. Crystal Chemistry and Surface Configurations of Two Iron-Bearing Trioctahedral Mica-1*M* Polytypes. *Clays Clay Miner.* **2014**, *62*, 243–252. [CrossRef]
49. Elmi, C.; Brigatti, M.F.; Guggenheim, S.; Pasquali, L.; Montecchi, M.; Malferrari, D.; Nannarone, S. Sodian Muscovite-2M1: Crystal Chemistry and Surface Features. *Can. Mineral.* **2013**, *51*, 5–14. [CrossRef]
50. Elmi, C.; Brigatti, M.F.; Guggenheim, S.; Pasquali, L.; Montecchi, M.; Nannarone, S. Crystal Chemistry and Surface Configurations of Two Polylithionite-1M Crystals. *Am. Mineral.* **2014**, *99*, 2049–2059. [CrossRef]
51. Adapa, S.; Swamy, D.R.; Kancharla, S.; Pradhan, S.; Malani, A. Role of Mono- and Divalent Surface Cations on the Structure and Adsorption Behavior of Water on Mica Surface. *Langmuir* **2018**, *34*, 14472–14488. [CrossRef]
52. Pintea, S.; de Poel, W.; de Jong, A.E.F.; Felici, R.; Vlieg, E. Solid–Liquid Interface Structure of Muscovite Mica in $SrCl_2$ and $BaCl_2$ Solutions. *Langmuir* **2018**, *34*, 4241–4248. [CrossRef] [PubMed]
53. Glausch, R. *Special Effect Pigments*; Vincentz: Hanover, Germany, 1998; ISBN 978-3-87870-541-3.
54. Gao, Q.; Wu, X.; Fan, Y.; Zhou, X. Low Temperature Synthesis and Characterization of Rutile TiO_2-Coated Mica–Titania Pigments. *Dye. Pigment.* **2012**, *95*, 534–539. [CrossRef]
55. Maile, F.J.; Pfaff, G.; Reynders, P. Effect Pigments—Past, Present and Future. *Prog. Org. Coat.* **2005**, *54*, 150–163. [CrossRef]
56. Ben Moshe, S.; Rytwo, G. Thiamine-Based Organoclay for Phenol Removal from Water. *Appl. Clay Sci.* **2018**, *155*, 50–56. [CrossRef]
57. Aslan, A.; Karaduman, E.; Derun, E.M.; Piskin, M.B. Development and Characterization of Negative Air Ion Emitting Mica- and Sericite-Based Antimicrobial Pearlescent Pigments. *Ceram. Int.* **2021**, *47*, 26421–26429. [CrossRef]
58. Tan, J.; Shen, L.; Fu, X.; Hou, W.; Chen, X. Preparation and Conductive Mechanism of Mica Titania Conductive Pigment. *Dye. Pigment.* **2004**, *62*, 107–114. [CrossRef]
59. Huang, Y.; Yang, Y.; Huan, W.; Yuan, H.; Wang, L.; Carlini, R. Preparation of Magnetic Pearlescent Pigment Mica/Fe_3O_4 by Thermally Decomposing Ferric Formate Composite Containing Hydrazine. *J. Inorg. Organomet. Polym.* **2018**, *28*, 651–670. [CrossRef]
60. Ryu, Y.C.; Kim, T.G.; Seo, G.-S.; Park, J.H.; Suh, C.S.; Park, S.-S.; Hong, S.-S.; Lee, G.D. Effect of Substrate on the Phase Transformation of TiO_2 in Pearlescent Pigment. *J. Ind. Eng. Chem.* **2008**, *14*, 213–218. [CrossRef]
61. Štengl, V.; Šubrt, J.; Bakardjieva, S.; Kalendova, A.; Kalenda, P. The Preparation and Characteristics of Pigments Based on Mica Coated with Metal Oxides. *Dye. Pigment.* **2003**, *58*, 239–244. [CrossRef]
62. Wang, Y.; Liu, Z.; Lu, X.; Lu, G.; Sun, J. Facile Synthesis of High Antistatic Mica-Titania@graphene Composite Pearlescent Pigment at Room Temperature. *Dye. Pigment.* **2017**, *145*, 436–443. [CrossRef]
63. Carroll, D. Ion Exchange in Clays and Other Minerals. *GSA Bull.* **1959**, *70*, 749–779. [CrossRef]
64. Awasthi, A.; Jadhao, P.; Kumari, K. Clay Nano-Adsorbent: Structures, Applications and Mechanism for Water Treatment. *SN Appl. Sci.* **2019**, *1*, 1076. [CrossRef]
65. Cavallaro, G.; Fakhrullin, R.; Pasbakhsh, P. Introduction: Overview of Nanoclays. In *Clay Nanoparticles*; Cavallaro, G., Fakhrullin, R., Pasbakhsh, P., Eds.; Elsevier: Amsterdam, The Netherlands, 2020; p. xv, ISBN 978-0-12-816783-0.
66. de Paiva, L.B.; Morales, A.R.; Valenzuela Díaz, F.R. Organoclays: Properties, Preparation and Applications. *Appl. Clay Sci.* **2008**, *42*, 8–24. [CrossRef]
67. He, H.; Ma, L.; Zhu, J.; Frost, R.L.; Theng, B.K.G.; Bergaya, F. Synthesis of Organoclays: A Critical Review and Some Unresolved Issues. *Appl. Clay Sci.* **2014**, *100*, 22–28. [CrossRef]
68. Pan, C.; Liu, P. Revisiting the Surface Olefin Cross-Metathesis of Nitrile Butadiene Rubber on Palygorskite Nanorods: Product Controlling for Specific Applications. *Appl. Clay Sci.* **2023**, *231*, 106757. [CrossRef]
69. Zhou, S.Q.; Niu, Y.Q.; Liu, J.H.; Chen, X.X.; Li, C.S.; Gates, W.P.; Zhou, C.H. Functional Montmorillonite/Polymer Coatings. *Clays Clay Miner.* **2022**, *70*, 209–232. [CrossRef]
70. Whitworth, T.M. Clay Minerals: Ion exchangeIon Exchange. In *Geochemistry*; Springer: Dordrecht, The Netherlands, 1998; pp. 85–87, ISBN 978-1-4020-4496-0.

71. Fang, B.; Lü, T.; Ning, F.; Pang, J.; He, Z.; Sun, J. Facilitating Gas Hydrate Dissociation Kinetics and Gas Migration in Clay Interlayer by Surface Cations Shielding Effects. *Fuel* **2022**, *318*, 123576. [CrossRef]
72. Zhou, C.; Tong, D.; Yu, W. 7—Smectite Nanomaterials: Preparation, Properties, and Functional Applications. In *Nanomaterials from Clay Minerals*; Wang, A., Wang, W., Eds.; Micro and Nano Technologies; Elsevier: Amsterdam, The Netherlands, 2019; pp. 335–364, ISBN 978-0-12-814533-3.
73. Appel, C.; Ma, L.Q.; Dean Rhue, R.; Kennelley, E. Point of Zero Charge Determination in Soils and Minerals via Traditional Methods and Detection of Electroacoustic Mobility. *Geoderma* **2003**, *113*, 77–93. [CrossRef]
74. Gao, W.; Zhao, S.; Wu, H.; Deligeer, W.; Asuha, S. Direct Acid Activation of Kaolinite and Its Effects on the Adsorption of Methylene Blue. *Appl. Clay Sci.* **2016**, *126*, 98–106. [CrossRef]
75. Li, G.; Cheng, W.; Jiang, T.; Sun, N.; Ai, L. Preparation of Porous Silica by Acid Dissociation of Thermally Activated Kaolinite. *Adv. Mater. Res.* **2011**, *284–286*, 1381–1384. [CrossRef]
76. Fida, H.; Guo, S.; Zhang, G. Preparation and Characterization of Bifunctional Ti–Fe Kaolinite Composite for Cr(VI) Removal. *J. Colloid Interface Sci.* **2015**, *442*, 30–38. [CrossRef] [PubMed]
77. Chang, P.; Yu, S.; Chen, T.; Ren, A.; Chen, C.; Wang, X. Effect of pH, Ionic Strength, Fulvic Acid and Humic Acid on Sorption of Th(IV) on Na-Rectorite. *J. Radioanal. Nucl. Chem.* **2007**, *274*, 153–160. [CrossRef]
78. Tan, X.L.; Chang, P.P.; Fan, Q.H.; Zhou, X.; Yu, S.M.; Wu, W.S.; Wang, X.K. Sorption of Pb(II) on Na-Rectorite: Effects of pH, Ionic Strength, Temperature, Soil Humic Acid and Fulvic Acid. *Colloids Surf. A Physicochem. Eng. Asp.* **2008**, *328*, 8–14. [CrossRef]
79. Dana, K.; Sarkar, M. 5—Organophilic Nature of Nanoclay. In *Clay Nanoparticles*; Cavallaro, G., Fakhrullin, R., Pasbakhsh, P., Eds.; Elsevier: Amsterdam, The Netherlands, 2020; pp. 117–138, ISBN 978-0-12-816783-0.
80. Kryuchkova, M.-B.; Batasheva, S.; Akhatova, F.; Babaev, V.; Buzyurova, D.; Vikulina, A.; Volodkin, D.; Fakhrullin, R.; Rozhina, E. Pharmaceuticals Removal by Adsorption with Montmorillonite Nanoclay Pharmaceuticals Removal by Adsorption with Montmorillonite Nanoclay. *Int. J. Mol. Sci.* **2021**, *22*, 9670. [CrossRef] [PubMed]
81. Liu, S.; Wu, P.; Yu, L.; Li, L.; Gong, B.; Zhu, N.; Dang, Z.; Yang, C. Preparation and Characterization of Organo-Vermiculite Based on Phosphatidylcholine and Adsorption of Two Typical Antibiotics. *Appl. Clay Sci.* **2017**, *137*, 160–167. [CrossRef]
82. Jacoby, M. As Nuclear Waste Piles up, Scientists Seek the Best Long-Term Storage Solutions. *Chem. Eng. News* **2020**, *98*, 12.
83. Sellin, P.; Leupin, O.X. The Use of Clay as an Engineered Barrier in Radioactive-Waste Management a Review. *Clays Clay Miner.* **2013**, *61*, 477–498. [CrossRef]
84. Wolthers, M.; Charlet, L.; Tournassat, C. Chapter 20—Reactivity of Bentonite: An Additive Model Applied to Uranyl Sorption. In *Interface Science and Technology*; Lützenkirchen, J., Ed.; Elsevier: Amsterdam, The Netherlands, 2006; Volume 11, pp. 539–552, ISBN 1573-4285.
85. Bildstein, O.; Claret, F. Chapter 5—Stability of Clay Barriers Under Chemical Perturbations. In *Developments in Clay Science*; Tournassat, C., Steefel, C.I., Bourg, I.C., Bergaya, F., Eds.; Natural and Engineered Clay Barriers; Elsevier: Amsterdam, The Netherlands, 2015; Volume 6, pp. 155–188.
86. Delage, P.; Cui, Y.J.; Tang, A.M. Clays in Radioactive Waste Disposal. *J. Rock Mech. Geotech. Eng.* **2010**, *2*, 111–123. [CrossRef]
87. Wersin, P.; Birgersson, M.; Olsson, S.; Karnland, O.; Snellman, M. Impact of Corrosion-Derived Iron on the Bentonite Buffer within the KBS-3H Disposal Concept—The Olkiluoto Site as Case Study. In *Olkiluoto Site as Case Study (No. SKB-R—08-34)*; Swedish Nuclear Fuel and Waste Management Co.: Oskarshamn, Sweden, 2008; p. 58.
88. Carlson, L.; Karnland, O.; Oversby, V.M.; Rance, A.P.; Smart, N.R.; Snellman, M.; Vähänen, M.; Werme, L.O. Experimental Studies of the Interactions between Anaerobically Corroding Iron and Bentonite. *Phys. Chem. Earth Parts A/B/C* **2007**, *32*, 334–345. [CrossRef]
89. Gorski, C.A.; Klüpfel, L.; Voegelin, A.; Sander, M.; Hofstetter, T.B. Redox Properties of Structural Fe in Clay Minerals. 2. Electrochemical and Spectroscopic Characterization of Electron Transfer Irreversibility in Ferruginous Smectite, SWa-1. *Environ. Sci. Technol.* **2012**, *46*, 9369–9377. [CrossRef]
90. Anastácio, A.S.; Aouad, A.; Sellin, P.; Fabris, J.D.; Bergaya, F.; Stucki, J.W. Characterization of a Redox-Modified Clay Mineral with Respect to Its Suitability as a Barrier in Radioactive Waste Confinement. *Appl. Clay Sci.* **2008**, *39*, 172–179. [CrossRef]
91. Wersin, P.; Jenni, A.; Mäder, U.K. Interaction of Corroding Iron with Bentonite in the ABM1 Experiment at Äspö, Sweden: A Microscopic Approach. *Clays Clay Miner.* **2015**, *63*, 51–68. [CrossRef]
92. Hadi, J.; Wersin, P.; Serneels, V.; Greneche, J.-M. Eighteen Years of Steel–Bentonite Interaction in the FEBEX in Situ Test at the Grimsel Test Site in Switzerland. *Clays Clay Miner.* **2019**, *67*, 111–131. [CrossRef]
93. Ongaro, G.; Pontefisso, A.; Zeni, E.; Lanero, F.; Famengo, A.; Zorzi, F.; Zaccariotto, M.; Galvanetto, U.; Fiorentin, P.; Gobbo, R.; et al. Chemical and Mechanical Characterization of Unprecedented Transparent Epoxy–Nanomica Composites—New Model Insights for Mechanical Properties. *Polymers* **2023**, *15*, 1456. [CrossRef] [PubMed]
94. Das, P.; Manna, S.; Behera, A.K.; Shee, M.; Basak, P.; Sharma, A.K. Current Synthesis and Characterization Techniques for Clay-Based Polymer Nano-Composites and Its Biomedical Applications: A Review. *Environ. Res.* **2022**, *212*, 113534. [CrossRef] [PubMed]
95. Liu, P. Polymer Modified Clay Minerals: A Review. *Appl. Clay Sci.* **2007**, *38*, 64–76. [CrossRef]
96. Franco-Urquiza, E.A. Clay-Based Polymer Nanocomposites: Essential Work of Fracture. *Polymers* **2021**, *13*, 2399. [CrossRef]
97. Ghanbari, A.; Behzadfar, E.; Arjmand, M. Properties of Talc Filled Reactor-Made Thermoplastic Polyolefin Composites. *J. Polym. Res.* **2019**, *26*, 241. [CrossRef]

98. Gozali Balkanloo, P.; Poursattar Marjani, A.; Zanbili, F.; Mahmoudian, M. Clay Mineral/Polymer Composite: Characteristics, Synthesis, and Application in Li-Ion Batteries: A Review. *Appl. Clay Sci.* **2022**, *228*, 106632. [CrossRef]
99. Gu, X.; Wang, Y.; Liu, X.; Zhang, S.; Li, H.; Sun, J.; Jin, X.; Tang, W. Efficient Approach to Enhancing the Fire Resistance of Polypropylene by Modified Microporous Aluminosilicate from Kaolinite as Synergist. *Polym. Adv. Technol.* **2020**, *31*, 1047–1058. [CrossRef]
100. Shehata, A.B.; Hassan, M.A.; Darwish, N.A. Kaolin Modified with New Resin–Iron Chelate as Flame Retardant System for Polypropylene. *J. Appl. Polym. Sci.* **2004**, *92*, 3119–3125. [CrossRef]
101. Sun, Y.; Yuan, B.; Chen, X.; Li, K.; Wang, L.; Yun, Y.; Fan, A. Suppression of Methane/Air Explosion by Kaolinite-Based Multi-Component Inhibitor. *Powder Technol.* **2019**, *343*, 279–286. [CrossRef]
102. Tang, W.; Zhang, S.; Sun, J.; Gu, X. Flame Retardancy and Thermal Stability of Polypropylene Composite Containing Ammonium Sulfamate Intercalated Kaolinite. *Ind. Eng. Chem. Res.* **2016**, *55*, 7669–7678. [CrossRef]
103. Tang, W.; Song, L.; Liu, F.; Dessie, W.; Qin, Z.; Zhang, S.; Gu, X. Improving the Flame Retardancy and Thermal Stability of Polypropylene Composites via Introducing Glycine Intercalated Kaolinite Compounds. *Appl. Clay Sci.* **2022**, *217*, 106411. [CrossRef]
104. Hu, Y.; Xu, T.; Xu, H.; Zhong, Y.; Zhang, L.; Wang, B.; Sui, X.; Feng, X.; Mao, Z. Preparation and Properties of Sepiolite-Based 3D Flame-Retardant Aerogel. *Clays Clay Miner.* **2023**, *70*, 865–881. [CrossRef]
105. Woo, S.H.; Lee, S.Y.; Yoon, Y.-G.; Rigacci, A.; Woo, J.-J.; Beauger, C.; Kim, H.-J. Functionalized Nanoclays for Improved Properties of Composite Proton Exchange Membranes. *J. Power Sources* **2022**, *549*, 232083. [CrossRef]
106. Azeez, A.A.; Rhee, K.Y.; Park, S.J.; Hui, D. Epoxy Clay Nanocomposites—Processing, Properties and Applications: A Review. *Compos. Part B Eng.* **2013**, *45*, 308–320. [CrossRef]
107. de Azeredo, H.M.C.; Otoni, C.G.; Assis, O.B.G.; Corrêa, D.S.; de Moura, M.R.; Mattoso, L.H.C. Nanoparticles and Antimicrobial Food Packaging. In *Reference Module in Food Science*; Elsevier: Amsterdam, The Netherlands, 2018; ISBN 978-0-08-100596-5.
108. Zaghouane-Boudiaf, H.; Boutahala, M. Preparation and Characterization of Organo-Montmorillonites. Application in Adsorption of the 2,4,5-Trichlorophenol from Aqueous Solution. *Adv. Powder Technol.* **2011**, *22*, 735–740. [CrossRef]
109. Zhu, J.; Qing, Y.; Wang, T.; Zhu, R.; Wei, J.; Tao, Q.; Yuan, P.; He, H. Preparation and Characterization of Zwitterionic Surfactant-Modified Montmorillonites. *J. Colloid Interface Sci.* **2011**, *360*, 386–392. [CrossRef]
110. Zhu, L.; Tian, S.; Zhu, J.; Shi, Y. Silylated Pillared Clay (SPILC): A Novel Bentonite-Based Inorgano–Organo Composite Sorbent Synthesized by Integration of Pillaring and Silylation. *J. Colloid Interface Sci.* **2007**, *315*, 191–199. [CrossRef]
111. Guo, Y.X.; Liu, J.H.; Gates, W.P.; Zhou, C.H. Organo-Modification of Montmorillonite. *Clays Clay Miner.* **2020**, *68*, 601–622. [CrossRef]
112. Amari, A.; Mohammed Alzahrani, F.; Mohammedsaleh Katubi, K.; Salem Alsaiari, N.; Tahoon, M.A.; Ben Rebah, F. Clay-Polymer Nanocomposites: Preparations and Utilization for Pollutants Removal. *Materials* **2021**, *14*, 1365. [CrossRef]
113. Hnamte, M.; Pulikkal, A.K. Clay-Polymer Nanocomposites for Water and Wastewater Treatment: A Comprehensive Review. *Chemosphere* **2022**, *307*, 135869. [CrossRef] [PubMed]
114. Trinh, B.M.; Chang, B.P.; Mekonnen, T.H. The Barrier Properties of Sustainable Multiphase and Multicomponent Packaging Materials: A Review. *Prog. Mater. Sci.* **2023**, *133*, 101071. [CrossRef]
115. Kim, J.-K.; Hu, C.; Woo, R.S.C.; Sham, M.-L. Moisture Barrier Characteristics of Organoclay–Epoxy Nanocomposites. *Compos. Sci. Technol.* **2005**, *65*, 805–813. [CrossRef]
116. Lange, J.; Wyser, Y. Recent Innovations in Barrier Technologies for Plastic Packaging—A Review. *Packag. Technol. Sci.* **2003**, *16*, 149–158. [CrossRef]
117. Merah, N.; Ashraf, F.; Shaukat, M.M. Mechanical and Moisture Barrier Properties of Epoxy–Nanoclay and Hybrid Epoxy–Nanoclay Glass Fibre Composites: A Review. *Polymers* **2022**, *14*, 1620. [CrossRef]
118. Pavlidou, S.; Papaspyrides, C.D. A Review on Polymer–Layered Silicate Nanocomposites. *Prog. Polym. Sci.* **2008**, *33*, 1119–1198. [CrossRef]
119. Ozkoc, G.; Kemaloglu, S.; Quaedflieg, M. Production of Poly(Lactic Acid)/Organoclay Nanocomposite Scaffolds by Microcompounding and Polymer/Particle Leaching. *Polym. Compos.* **2010**, *31*, 674–683. [CrossRef]
120. Kalendova, A.; Merinska, D.; Gerard, J.F.; Slouf, M. Polymer/Clay Nanocomposites and Their Gas Barrier Properties. *Polym. Compos.* **2013**, *34*, 1418–1424. [CrossRef]
121. Raquez, J.-M.; Habibi, Y.; Murariu, M.; Dubois, P. Polylactide (PLA)-Based Nanocomposites. *Prog. Polym. Sci.* **2013**, *38*, 1504–1542. [CrossRef]
122. Farah, S.; Anderson, D.G.; Langer, R. Physical and Mechanical Properties of PLA, and Their Functions in Widespread Applications—A Comprehensive Review. *Adv. Drug Deliv. Rev.* **2016**, *107*, 367–392. [CrossRef]
123. Singha, S.; Hedenqvist, M.S. A Review on Barrier Properties of Poly(Lactic Acid)/Clay Nanocomposites. *Polymers* **2020**, *12*, 1095. [CrossRef] [PubMed]
124. Zhang, Y.; Deng, J.; Shao, Y.; Shi, Q.; Meng, G.; Ping, L. Effect of Polyaniline/Organophilic Montmorillonite Composites on Properties of Epoxy Coating. *Corros. Rev.* **2014**, *32*, 227–236. [CrossRef]
125. Lira, E.; Salazar, F.N.; Rodríguez-Bencomo, J.J.; Vincenzi, S.; Curioni, A.; López, F. Effect of Using Bentonite during Fermentation on Protein Stabilisation and Sensory Properties of White Wine. *Int. J. Food Sci. Technol.* **2014**, *49*, 1070–1078. [CrossRef]

126. Jaeckels, N.; Tenzer, S.; Meier, M.; Will, F.; Dietrich, H.; Decker, H.; Fronk, P. Influence of Bentonite Fining on Protein Composition in Wine. *LWT* **2017**, *75*, 335–343. [CrossRef]
127. Ubeda, C.; Lambert-Royo, M.I.; Gil i Cortiella, M.; Del Barrio-Galán, R.; Peña-Neira, Á. Chemical, Physical, and Sensory Effects of the Use of Bentonite at Different Stages of the Production of Traditional Sparkling Wines. *Foods* **2021**, *10*, 390. [CrossRef]
128. Blade, W.H.; Boulton, R. Adsorption of Protein by Bentonite in a Model Wine Solution. *Am. J. Enol. Vitic.* **1988**, *39*, 193–199. [CrossRef]
129. Cosme, F.; Fernandes, C.; Ribeiro, T.; Filipe-Ribeiro, L.; Nunes, F.M. White Wine Protein Instability: Mechanism, Quality Control and Technological Alternatives for Wine Stabilisation—An Overview. *Beverages* **2020**, *6*, 19. [CrossRef]
130. Sauvage, F.-X.; Bach, B.; Moutounet, M.; Vernhet, A. Proteins in White Wines: Thermo-Sensitivity and Differential Adsorbtion by Bentonite. *Food Chem.* **2010**, *118*, 26–34. [CrossRef]
131. Lucchetta, M.; Pocock, K.F.; Waters, E.J.; Marangon, M. Use of Zirconium Dioxide during Fermentation as an Alternative to Protein Fining with Bentonite for White Wines. *Am. J. Enol. Vitic.* **2013**, *64*, 400–404. [CrossRef]
132. Sommer, S.; Sommer, S.J.; Gutierrez, M. Characterization of Different Bentonites and Their Properties as a Protein-Fining Agent in Wine. *Beverages* **2022**, *8*, 31. [CrossRef]
133. Jackson, R.S. 8—Postfermentation Treatments and Related Topics. In *Wine Science*, 3rd ed.; Jackson, R.S., Ed.; Academic Press: San Diego, CA, USA, 2008; pp. 418–519, ISBN 978-0-12-373646-8.
134. Marchal, R.; Waters, E.J. 7—New Directions in Stabilization, Clarification and Fining of White Wines. In *Managing Wine Quality*; Reynolds, A.G., Ed.; Woodhead Publishing: Sawston, UK, 2010; pp. 188–225, ISBN 978-1-84569-798-3.
135. Weiss, K.C.; Lange, L.W.; Bisson, L.F. Small-Scale Fining Trials: Effect of Method of Addition on Efficiency of Bentonite Fining. *Am. J. Enol. Vitic.* **2001**, *52*, 275–279. [CrossRef]
136. Lambri, M.; Dordoni, R.; Silva, A.; Faveri, D.M.D. Odor-Active Compound Adsorption onto Bentonite in a Model White Wine Solution. *Chem. Eng. Trans.* **2013**, *32*, 1741–1746.
137. Catarino, S.; Madeira, M.; Monteiro, F.; Rocha, F.; Curvelo-Garcia, A.S.; de Sousa, R.B. Effect of Bentonite Characteristics on the Elemental Composition of Wine. *J. Agric. Food Chem.* **2008**, *56*, 158–165. [CrossRef]
138. Sommer, S.; Tondini, F. Sustainable Replacement Strategies for Bentonite in Wine Using Alternative Protein Fining Agents. *Sustainability* **2021**, *13*, 1860. [CrossRef]
139. Viseras, C.; Sánchez-Espejo, R.; Palumbo, R.; Liccardi, N.; García-Villén, F.; Borrego-Sánchez, A.; Massaro, M.; Riela, S.; López-Galindo, A. Clays in Cosmetics and Personal-Care Products. *Clays Clay Miner.* **2021**, *69*, 561–575. [CrossRef]
140. Bastos, C.M.; Rocha, F. Assessment of Some Clay-Based Products Available on Market and Designed for Topical Use. *Geosciences* **2022**, *12*, 453. [CrossRef]
141. Massaro, M.; Colletti, C.; Lazzara, G.; Riela, S. The Use of Some Clay Minerals as Natural Resources for Drug Carrier Applications. *JFB* **2018**, *9*, 58. [CrossRef]
142. Shahbaz, A.; Hussain, N.; Mahmood, T.; Iqbal, H.M.N.; Bin Emran, T.; Show, P.L.; Bilal, M. 17—Polymer Nanocomposites for Biomedical Applications. In *Smart Polymer Nanocomposites*; Ali, N., Bilal, M., Khan, A., Nguyen, T.A., Gupta, R.K., Eds.; Micro and Nano Technologies; Elsevier: Amsterdam, The Netherlands, 2023; pp. 379–394, ISBN 978-0-323-91611-0.
143. Perioli, L.; Ambrogi, V.; Bertini, B.; Ricci, M.; Nocchetti, M.; Latterini, L.; Rossi, C. Anionic Clays for Sunscreen Agent Safe Use: Photoprotection, Photostability and Prevention of Their Skin Penetration. *Eur. J. Pharm. Biopharm.* **2006**, *62*, 185–193. [CrossRef]
144. Kim, D.; Kim, D.; Kim, J.; Park, C.; Roh, K.-M.; Kang, I.-M.; Seo, S.M. Synthesis and Characterization Fo Montmorillonite Supported TiO_2 Composites for Enhanced UV Absorption. *Clays Clay Miner.* **2020**, *68*, 533–543. [CrossRef]
145. Aguzzi, C.; Cerezo, P.; Viseras, C.; Caramella, C. Use of Clays as Drug Delivery Systems: Possibilities and Limitations. *Appl. Clay Sci.* **2007**, *36*, 22–36. [CrossRef]
146. Del Hoyo, C. Layered Double Hydroxides and Human Health: An Overview. *Appl. Clay Sci.* **2007**, *36*, 103–121. [CrossRef]
147. Wanna, D.; Alam, C.; Toivola, D.M.; Alam, P. Bacterial Cellulose–Kaolin Nanocomposites for Application as Biomedical Wound Healing Materials. *Adv. Nat. Sci Nanosci. Nanotechnol.* **2013**, *4*, 045002. [CrossRef]
148. Williams, L.B.; Haydel, S.E. Evaluation of the Medicinal Use of Clay Minerals as Antibacterial Agents. *Int. Geol. Rev.* **2010**, *52*, 745–770. [CrossRef]
149. Samlíková, M.; Holešová, S.; Hundáková, M.; Pazdziora, E.; Jankovič, Ľ.; Valášková, M. Preparation of Antibacterial Chlorhexidine/Vermiculite and Release Study. *Int. J. Miner. Process.* **2017**, *159*, 1–6. [CrossRef]
150. Viseras, C.; Carazo, E.; Borrego-Sánchez, A.; García-Villén, F.; Sánchez-Espejo, R.; Cerezo, P.; Aguzzi, C. Clay Minerals in Skin Drug Delivery. *Clays Clay Miner.* **2019**, *67*, 59–71. [CrossRef]
151. Khatoon, N.; Chu, M.Q.; Zhou, C.H. Nanoclay-Based Drug Delivery Systems and Their Therapeutic Potentials. *J. Mater. Chem. B* **2020**, *8*, 7335–7351. [CrossRef]
152. Guggenheim, S. An Overview of Order/Disorder in Hydrous Phyllosilicates. In *Layered Mineral Structures and Their Application in Advanced Technologies*; Brigatti, M.F., Mottana, A., Eds.; Mineralogical Society of Great Britain and Ireland: Middlesex, UK, 2011; Volume 11, pp. 72–111, ISBN 978-0-903056-29-8.
153. Tournassat, C.; Greneche, J.-M.; Tisserand, D.; Charlet, L. The Titration of Clay Minerals: I. Discontinuous Backtitration Technique Combined with CEC Measurements. *J. Colloid Interface Sci.* **2004**, *273*, 224–233. [CrossRef]
154. Rebitski, E.P.; Darder, M.; Sainz-Diaz, C.I.; Carraro, R.; Aranda, P.; Ruiz-Hitzky, E. Theoretical and Experimental Investigation on the Intercalation of Metformin into Layered Clay Minerals. *Appl. Clay Sci.* **2020**, *186*, 105418. [CrossRef]

155. Peixoto, D.; Pereira, I.; Pereira-Silva, M.; Veiga, F.; Hamblin, M.R.; Lvov, Y.; Liu, M.; Paiva-Santos, A.C. Emerging Role of Nanoclays in Cancer Research, Diagnosis, and Therapy. *Coord. Chem. Rev.* **2021**, *440*, 213956. [CrossRef]
156. Chakraborty, J.; Chakraborty, M.; Ghosh, S.; Mitra, M.K. Drug Delivery Using Nanosized Layered Double Hydroxide, an Anionic Clay. *KEM* **2013**, *571*, 133–167. [CrossRef]
157. Kumari, S.; Thakur, N.; Kumar, R.; Thakur, R.C.; Sharma, A. Effect of Synthetic Parameters on Crystallinity of Hydrotalcite-Like Anionic Clays with Elucidation and Identification through X-ray Diffraction Analysis. *ECS Trans.* **2022**, *107*, 18903–18921. [CrossRef]
158. Mei, X.; Wang, W.; Yan, L.; Hu, T.; Liang, R.; Yan, D.; Wei, M.; Evans, D.G.; Duan, X. Hydrotalcite Monolayer toward High Performance Synergistic Dual-Modal Imaging and Cancer Therapy. *Biomaterials* **2018**, *165*, 14–24. [CrossRef] [PubMed]